ON THE NUMERICAL EVALUATION OF DISTRIBUTIONS
IN RANDOM MATRIX THEORY: A REVIEW

FOLKMAR BORNEMANN

ABSTRACT. In this paper we review and compare the numerical evaluation of those probability distributions in random matrix theory that are analytically represented in terms of Painlevé transcendents or Fredholm determinants. Concrete examples for the Gaussian and Laguerre (Wishart) β-ensembles and their various scaling limits are discussed. We argue that the numerical approximation of Fredholm determinants is the conceptually more simple and efficient of the two approaches, easily generalized to the computation of joint probabilities and correlations. Having the means for extensive numerical explorations at hand, we discovered new and surprising determinantal formulae for the k-th largest (or smallest) level in the edge scaling limits of the Orthogonal and Symplectic Ensembles; formulae that in turn led to improved numerical evaluations. The paper comes with a toolbox of Matlab functions that facilitates further mathematical experiments by the reader.

1. INTRODUCTION

Random Matrix Theory (RMT) has found many applications, most notably in physics, multivariate statistics, electrical engineering, and finance. As soon as there is the need for specific numbers, such as moments, quantiles, or correlations, the actual numerical evaluation of the underlying probability distributions becomes of interest. Without additional structure there would be, in general, only one method: Monte Carlo simulation. However, because of the universality of certain scaling limits (for a review see, e.g., Deift 2007), a family of distinguished distribution functions enters which is derived from highly structured matrix models enjoying closed analytic solutions. These functions constitute a new class of special functions comparable in import to the classic distributions of probability theory. This paper addresses the accurate numerical evaluation[1] of many of these functions on the one hand and shows, on the other hand, that such work facilitates numerical explorations that may lead, in the sense of Experimental Mathematics (Borwein and Bailey 2004), to new theoretical discoveries, see the results of Section 6.

1.1. **The Common Point of View.** The closed analytic solutions alluded to above are based (for deeper reasons or because of contingency) on two concurrent tools: Fredholm determinants of integral operators and Painlevé transcendents. Concerning the question which of them is better suited to be attacked numerically, there has been a prevailing point of view for the last 15 years or so, explicitly formulated by Tracy and Widom (2000, Footnote 10): "Without the Painlevé representation,

---

[1]Limiting the means, as customary in numerical analysis for reasons of efficiency and strict adherence to numerical stability, to IEEE double precision hardware arithmetic (about 16 digits precision).

the numerical evaluation of the Fredholm determinants is quite involved." To understand the possible genesis of this point of view let us recall the results for the two most important scaling limits of the Gaussian Unitary Ensemble (GUE).

1.1.1. *Level Spacing Function of GUE.* The large matrix limit of GUE, scaled for level spacing 1 in the bulk, yields the function

$$E_2(0;s) = \mathbb{P}(\text{no levels lie in } (0,s)). \tag{1.1}$$

Gaudin (1961) showed that this function can be represented as a Fredholm determinant, namely,[2]

$$E_2(0;s) = \det\left(I - K_{\sin}\!\restriction_{L^2(0,s)}\right), \qquad K_{\sin}(x,y) = \text{sinc}(\pi(x-y)). \tag{1.2}$$

He proceeded by showing that the eigenfunctions of this selfadjoint integral operator are the radial prolate spheroidal wave functions with certain parameters. Using tables (Stratton, Morse, Chu, Little and Corbató 1956) of these special functions he was finally able to evaluate $E_2(0;s)$ numerically.[3] On the other hand, in an admirably intricate analytic tour de force Jimbo, Miwa, Môri and Sato (1980) expressed the Fredholm determinant by

$$E_s(0;s) = \exp\left(-\int_0^{\pi s} \frac{\sigma(x)}{x}\,dx\right) \tag{1.3}$$

in terms of the Jimbo–Miwa–Okamoto σ-form of Painlevé V, namely

$$(x\sigma_{xx})^2 = 4(\sigma - x\sigma_x)(x\sigma_x - \sigma - \sigma_x^2), \qquad \sigma(x) \simeq \frac{x}{\pi} + \frac{x^2}{\pi^2} \quad (x \to 0). \tag{1.4}$$

1.1.2. *The Tracy–Widom distribution.* The large matrix limit of GUE, scaled for the fluctuations at the soft edge (that is, the maximum eigenvalue), yields the function

$$F_2(s) = \mathbb{P}(\text{no levels lie in } (s,\infty)). \tag{1.5}$$

Implicitly known for quite some time (see, e.g., Bronk 1964, Brézin and Kazakov 1990, Moore 1990), the determinantal representation

$$F_2(s) = \det\left(I - K_{\text{Ai}}\!\restriction_{L^2(s,\infty)}\right), \qquad K_{\text{Ai}}(x,y) = \frac{\text{Ai}(x)\text{Ai}'(y) - \text{Ai}'(x)\text{Ai}(y)}{x-y}, \tag{1.6}$$

was spelt out by Forrester (1993) and by Tracy and Widom (1993b). The search for an analogue to Gaudin's method remained unsuccessful since there is no solution of the corresponding eigenvalue problem known in terms of classic

---

[2]We use the same symbol K to denote both, the integral operator $K\!\restriction_X$ acting on the Hilbert space X and its kernel function $K(x,y)$.

[3]Strictly speaking Gaudin (1961) was concerned with evaluating the level spacing function $E_1(0;s)$ of GOE that he represented as the Fredholm determinant of the even sine kernel, see (5.8a) below. However, the extension of Gaudin's method to $E_2(0;s)$ is fairly straightforward, see Dyson (1962) for a determinantal formula that is equivalent to (1.2), namely (5.7) with $k = 0$, and Kahn (1963) for subsequent numerical work. As was pointed out by Odlyzko (1987, p. 305), who himself had calculated $E_2(0;s)$ by Gaudin's method using Van Buren's implementation of the prolate wave functions, Kahn's tables, reproduced in the first 1967 edition of Mehta's book, are rather inaccurate. In contrast, the tables in Mehta and des Cloizeaux (1972), reproduced in the second 1991 and third 2002 edition of Mehta's book, are basically accurate *with the proviso* that the arguments have to be read not as the displayed four digit numbers but rather as $s = 2t/\pi$ with $t = 0.0, 0.1, 0.2, 0.3$, etc. A modern implementation of Gaudin's method for $E_2(0;s)$, using Mathematica's fairly recent ability to evaluate the prolate wave functions, can be found in Bornemann (2010a, §7.1).

special functions (Mehta 2004, p. 453). It was therefore a major breakthrough when Tracy and Widom (1993b, 1994a) derived their now famous representation

$$F_2(s) = \exp\left(-\int_s^\infty (x-s)u(x)^2\,dx\right) \tag{1.7}$$

in terms of the Hastings–McLeod (1980) solution $u(x)$ of Painlevé II, namely

$$u_{xx} = 2u^3 + xu, \qquad u(x) \simeq \mathrm{Ai}(x) \quad (x \to \infty). \tag{1.8}$$

Subsequent numerical evaluations were then, until the recent work of Bornemann (2010a), exclusively based on solving this asymptotic initial value problem.

1.2. **Challenging the Common Point of View.** In this paper we challenge the common point of view that a Painlevé representation would be, at least numerically, preferable to a Fredholm determinant formula. We do so from the following angles: Simplicity, efficiency, accuracy, and extendibility. Let us briefly indicate the rationale for our point of view.

(1) The numerical evaluation of Painlevé transcendents encountered in RMT is more involved as one would think at first sight. For reasons of numerical stability one needs additional, deep analytic knowledge, namely, asymptotic expansions of the corresponding connection formulae (see Section 3).

(2) There is an extremely simple, fast, accurate, and *general* numerical method for evaluating Fredholm determinants (see Section 4).

(3) Multivariate functions such as joint probability distributions often have a representation by a Fredholm determinant (see Section 8). On the other hand, if available at all, a representation in terms of a nonlinear *partial* differential equation is of very limited numerical use right now.

1.3. **Outline of the Paper.** In Section 2 we collect some fundamental functions of RMT whose numerical solutions will play a role in the sequel. The intricate issues of a numerical solution of the Painlevé transcendents encountered in RMT are subject of Section 3. An exposition of Bornemann's (2010a) method for the numerical evaluation of Fredholm determinants is given in Section 4. The numerical evaluation of the k-level spacings in the bulk of GOE, GUE, and GSE, by using Fredholm determinants, is addressed in Section 5. In Section 6 we get to new determinantal formulae for the distributions of the k-th largest level in the soft edge scaling limit of GOE and GSE. These formulae rely on a determinantal identity that we found by extensive numerical experiments before proving it. By a powerful structural analogy, in Section 7 these formulae are easily extended to the k-th smallest level in the hard edge scaling limit of LOE and LSE. In Section 8, we discuss some examples of joint probabilities, like the one for the largest two eigenvalues of GUE at the soft edge or the one of the Airy process for two different times. Finally, in Section 9, we give a short introduction into using the Matlab toolbox that comes with this paper.

2. Some Distribution Functions of RMT and Their Representation

In this section we collect some fundamental functions of RMT whose numerical evaluation will explicitly be discussed in the sequel. We do not strive for completeness here; but we will give sufficiently many examples to be able to judge of simplicity and generality of the numerical approaches later on.

We confine ourselves to the Gaussian (Hermite) and Laguerre (Wishart) ensembles. That is, we consider $n \times n$ random matrix ensembles with real (nonnegative in the case of the Laguerre ensemble) spectrum such that the joint probability distribution of its (unordered) eigenvalues is given by

$$p(x_1, \ldots, x_n) = c \prod_i w(x_i) \cdot \prod_{i<j} |x_i - x_j|^\beta. \tag{2.1}$$

Here, β takes the values 1, 2, or 4 (Dyson's "three fold way"). The weight function $w(x)$ will be either a Gaussian or, in the case of the Laguerre ensembles, a function of the type $w_\alpha(x) = x^\alpha e^{-x}$ $(\alpha > -1)$.

2.1. **Gaussian Ensembles.** Here, we take the Gaussian weight functions[4]

- $w(x) = e^{-x^2/2}$ for $\beta = 1$, the Gaussian Orthogonal Ensemble (GOE),

- $w(x) = e^{-x^2}$ for $\beta = 2$, the Gaussian Unitary Ensemble (GUE),

- $w(x) = e^{-x^2}$ for $\beta = 4$, the Gaussian Symplectic Ensemble (GSE).

We define, for an open interval $J \subset \mathbb{R}$, the basic quantity

$$E_\beta^{(n)}(k; J)$$

$$= \mathbb{P}\left(\text{exactly } k \text{ eigenvalues of the } n \times n \text{ Gaussian } \beta\text{-ensemble lie in } J\right). \tag{2.2}$$

More general quantities will be considered in Section 8.3.

2.1.1. *Scaling limits.* The *bulk scaling* limit is given by (see Mehta 2004, §§6.3, 7.2, and 11.7)

$$E_\beta^{(\text{bulk})}(k; J) = \begin{cases} \lim_{n\to\infty} E_\beta^{(n)}(k; \pi\, 2^{-1/2} n^{-1/2} J) & \beta = 1 \text{ or } \beta = 2, \\ \lim_{n\to\infty} E_\beta^{(n)}(k; \pi\, n^{-1/2} J) & \beta = 4. \end{cases} \tag{2.3}$$

The *soft edge scaling* limit is given by (see Forrester and Rains 2001, p. 194)

$$E_\beta^{(\text{soft})}(k; J) = \begin{cases} \lim_{n\to\infty} E_\beta^{(n)}(k; \sqrt{2n} + 2^{-1/2} n^{-1/6} J) & \beta = 1 \text{ or } \beta = 2, \\ \lim_{n\to\infty} E_\beta^{(n/2)}(k; \sqrt{2n} + 2^{-1/2} n^{-1/6} J) & \beta = 4. \end{cases} \tag{2.4}$$

---

[4]We follow Forrester and Rains (2001) in the choice of the variances of the Gaussian weights. Note that Mehta (2004, Chap. 3), such as Tracy and Widom in most of their work, uses $w(x) = e^{-\beta x^2/2}$. However, one has to be alert: from p. 175 onwards, Mehta uses $w(x) = e^{-x^2}$ for $\beta = 4$ in his book, too.

2.1.2. *Level spacing.* The k-level spacing function $E_\beta(k;s)$ of Mehta (2004, §6.1.2) is

$$E_\beta(k;s) = E_\beta^{(\text{bulk})}(k;(0,s)). \tag{2.5}$$

The k-level spacing density $p_\beta(k;s)$, that is, the probability density of the distance of a level in the bulk to its $(k+1)$-st next neighbor is (see Mehta 2004, Eq. (6.1.18))

$$p_\beta(k;s) = \frac{d^2}{ds^2} \sum_{j=0}^{k} (k+1-j) E_\beta(j;s) \qquad (k = 0,1,2,\ldots). \tag{2.6}$$

Since the bulk scaling limit was made such that the expected distance between neighboring eigenvalues is one, we have (see Mehta 2004, Eq. (6.1.26))

$$\int_0^\infty p_\beta(k;s) = 1, \qquad \int_0^\infty s p_\beta(k;s)\,ds = k+1. \tag{2.7}$$

Likewise, there holds for $s \geqslant 0$

$$\sum_{k=0}^{\infty} E_\beta(k;s) = 1, \qquad \sum_{k=0}^{\infty} k E_\beta(k;s) = s; \tag{2.8}$$

see, e.g., Mehta (2004, Eqs. (6.1.19/20)) or Deift (1999b, p. 119). Such constraints are convenient means to assess the accuracy of numerical methods (see Examples 9.3.2/9.4.2 and, for a generalization, Example 9.3.3).

2.1.3. *Distribution of the k-th largest eigenvalue.* The cumulative distribution function of the k-th largest eigenvalue is, in the soft edge scaling limit,

$$F_\beta(k;s) = \sum_{j=0}^{k-1} E_\beta^{(\text{soft})}(j;(s,\infty)). \tag{2.9}$$

The famous Tracy–Widom (1996) distributions $F_\beta(s)$ are given by

$$F_\beta(s) = \begin{cases} F_\beta(1;s) & \beta = 1 \text{ or } \beta = 2, \\ F_\beta(1;\sqrt{2}\,s) & \beta = 4. \end{cases} \tag{2.10}$$

2.2. **Determinantal Representations for Gaussian Ensembles.**

2.2.1. *GUE.* Here, the basic formula is (see Deift 1999b, §5.4)

$$E_2^{(n)}(k;J) = \frac{(-1)^k}{k!} \frac{d^k}{dz^k} D_2^{(n)}(z;J) \Big|_{z=1}, \tag{2.11a}$$

$$D_2^{(n)}(z;J) = \det\left(1 - z\,K_n{\upharpoonright}_{L^2(J)}\right), \tag{2.11b}$$

with the Hermite kernel (the second form follows from Christoffel–Darboux)

$$K_n(x,y) = \sum_{k=0}^{n-1} \phi_k(x)\phi_k(y) = \sqrt{\frac{n}{2}} \frac{\phi_n(x)\phi_{n-1}(y) - \phi_{n-1}(x)\phi_n(y)}{x-y} \tag{2.12}$$

that is built from the $L^2(\mathbb{R})$-orthonormal system of the Hermite functions

$$\phi_k(x) = \frac{e^{-x^2/2} H_k(x)}{\pi^{1/4}\sqrt{k!}\,2^{k/2}}. \tag{2.13}$$

The bulk scaling limit is given by (see Mehta 2004, §A.10)

$$E_2^{(\text{bulk})}(k; J) = \frac{(-1)^k}{k!} \frac{d^k}{dz^k} D_2^{(\text{bulk})}(z; J)\bigg|_{z=1}, \tag{2.14a}$$

$$D_2^{(\text{bulk})}(z; J) = \det\left(1 - z\, K_{\sin}\!\restriction_{L^2(J)}\right), \tag{2.14b}$$

with the sine kernel $K_{\sin}$ defined in (1.2). The soft edge scaling limit is given by (see Forrester 1993, §3.1)

$$E_2^{(\text{soft})}(k; J) = \frac{(-1)^k}{k!} \frac{d^k}{dz^k} D_2^{(\text{soft})}(z; J)\bigg|_{z=1}, \tag{2.15a}$$

$$D_2^{(\text{soft})}(z; J) = \det\left(1 - z\, K_{\text{Ai}}\!\restriction_{L^2(J)}\right), \tag{2.15b}$$

with the Airy kernel K_{Ai} defined in (1.6).

2.2.2. *GSE.* Using Dyson's quaternion determinants one can find a determinantal formula for $E_4^{(n)}(k; J)$ which involves a finite rank matrix kernel (see Mehta 2004, Chap. 8)—a formula that is amenable to the numerical methods of Section 4. We confine ourselves to the soft edge scaling limit of this formula which yields (Tracy and Widom 2005)

$$E_4^{(\text{soft})}(k; J) = \frac{(-1)^k}{k!} \frac{d^k}{dz^k} \sqrt{D_4(z; J)}\bigg|_{z=1}, \tag{2.16a}$$

where the entries of the matrix kernel determinant

$$D_4(z; J) = \det\left(I - \frac{z}{2} \begin{pmatrix} S & SD \\ IS & S^* \end{pmatrix}\!\restriction_{L^2(J) \oplus L^2(J)}\right) \tag{2.16b}$$

are given by (with the adjoint kernel $S^*(x, y) = S(y, x)$ obtained from transposition)

$$S(x, y) = K_{\text{Ai}}(x, y) - \frac{1}{2}\text{Ai}(x) \int_y^\infty \text{Ai}(\eta)\, d\eta, \tag{2.17a}$$

$$SD(x, y) = -\partial_y K_{\text{Ai}}(x, y) - \frac{1}{2}\text{Ai}(x)\text{Ai}(y), \tag{2.17b}$$

$$IS(x, y) = -\int_x^\infty K_{\text{Ai}}(\xi, y)\, d\xi + \frac{1}{2}\int_x^\infty \text{Ai}(\xi)\, d\xi \int_y^\infty \text{Ai}(\eta)\, d\eta. \tag{2.17c}$$

Albeit this expression is also amenable to the numerical methods of Section 4, we will discuss, for the significant special cases

$$E_4^{(\text{bulk})}(k; (0, s)) \quad \text{and} \quad E_4^{(\text{soft})}(k; (s, \infty)), \tag{2.18}$$

alternative determinantal formulae that are far more efficient numerically, see Section 5 and Section 6, respectively.

2.2.3. *GOE.* There are also determinantal formulae for $E_1^{(\text{bulk})}(k; J)$ and its various scaling limits, see Mehta (2004, Chap. 7) and Tracy and Widom (2005). However, these determinantal formulae are based on matrix kernels that involve a *discontinuous* term. To be specific we recall the result for the soft edge scaling limit:

$$E_1^{(\text{soft})}(k; J) = \frac{(-1)^k}{k!} \frac{d^k}{dz^k} \left. \sqrt{D_1(z; J)} \right|_{z=1}, \tag{2.19a}$$

where the entries of the matrix kernel determinant

$$D_1(z; J) = \det\left(I - z \begin{pmatrix} S & SD \\ IS_\epsilon & S^* \end{pmatrix} \upharpoonright_{X_1(J) \oplus X_2(J)} \right) \tag{2.19b}$$

are given by (with the adjoint kernel $S^*(x, y) = S(y, x)$ obtained from transposition)

$$S(x, y) = K_{\text{Ai}}(x, y) + \frac{1}{2}\text{Ai}(x)\left(1 - \int_y^\infty \text{Ai}(\eta)\, d\eta\right), \tag{2.20a}$$

$$SD(x, y) = -\partial_y K_{\text{Ai}}(x, y) - \frac{1}{2}\text{Ai}(x)\text{Ai}(y), \tag{2.20b}$$

$$IS_\epsilon(x, y) = -\epsilon(x - y) - \int_x^\infty K_{\text{Ai}}(\xi, y)\, d\xi$$
$$+ \frac{1}{2}\left(\int_y^x \text{Ai}(\xi)\, d\xi + \int_x^\infty \text{Ai}(\xi)\, d\xi \int_y^\infty \text{Ai}(\eta)\, d\eta\right). \tag{2.20c}$$

with the *discontinuous* function

$$\epsilon(x) = \tfrac{1}{2}\text{sign}(x). \tag{2.20d}$$

This discontinuity poses considerable difficulties for the proper theoretical justification of the operator determinant: for appropriately chosen weighted L^2 spaces $X_1(J)$ and $X_2(J)$, the matrix kernel operator is a Hilbert–Schmidt operator with a trace class diagonal and the determinant has to be understood as a Hilbert–Carleman regularized determinant (see Tracy and Widom 2005, p. 2199). Moreover, it renders the unmodified numerical methods of Section 4 rather inefficient. Nevertheless, for the significant special cases

$$E_1^{(\text{bulk})}(k; (0, s)) \quad \text{and} \quad E_1^{(\text{soft})}(k; (s, \infty)) \tag{2.21}$$

there are alternative determinantal formulae, which are amenable to an efficient numerical evaluation, see Section 5 and Section 6, respectively.

2.3. **Painlevé Representations for Gaussian Ensembles.** For the important family of *integrable* kernels (see Deift 1999a), Tracy and Widom (1993a, 1993b, 1994a, 1994c) found a general method to represent determinants of the form

$$\det\left(I - zK\upharpoonright_{L^2(a,b)} \right) \tag{2.22}$$

explicitly by a system of partial differential equations with respect to the independent variables a and b. Fixing one of the bounds yields an ordinary differential equation (that notwithstanding depends on the fixed bound). In RMT, this ordinary differential equation turned out, case by case, to be a Painlevé equation.

The typical choices of intervals with a fixed bound are $J = (0, s)$ or $J = (s, \infty)$, depending on whether one looks at the bulk or the soft edge of the spectrum.

2.3.1. *GUE.* Tracy and Widom (1994c) calculated, for the determinant (2.11b) with $J = (s, \infty)$, the representation

$$D_2^{(n)}(z; (s, \infty)) = \exp\left(-\int_s^\infty \sigma(x; z)\, dx\right) \tag{2.23}$$

in terms of the Jimbo–Miwa–Okamoto σ-form of Painlevé IV, namely

$$\sigma_{xx}^2 = 4(\sigma - x\sigma_x)^2 - 4\sigma_x^2(\sigma_x + 2n), \tag{2.24a}$$

$$\sigma(x; z) \simeq z \frac{2^{n-1} x^{2n-2}}{\sqrt{\pi}\, \Gamma(n)} e^{-x^2} \qquad (x \to \infty). \tag{2.24b}$$

As mentioned in the introduction, for the determinant (2.14b) and $J = (0, s)$, Jimbo et al. (1980) found the representation (see also Tracy and Widom 1993a, Thm. 9)

$$D_2^{(\text{bulk})}(z; (0, s)) = \exp\left(-\int_0^{\pi s} \frac{\sigma(x; z)}{x}\, dx\right) \tag{2.25}$$

in terms of the Jimbo–Miwa–Okamoto σ-form of Painlevé V, namely

$$(x\sigma_{xx})^2 = 4(\sigma - x\sigma_x)(x\sigma_x - \sigma - \sigma_x^2), \tag{2.26a}$$

$$\sigma(x; z) \simeq \frac{z}{\pi} x + \frac{z^2}{\pi^2} x^2 \qquad (x \to 0). \tag{2.26b}$$

Finally, there is Tracy and Widom's (1993b, 1994a) famous representation of the determinant (2.15b) for $J = (s, \infty)$,

$$D_2^{(\text{soft})}(z; (s, \infty)) = \exp\left(-\int_s^\infty (x - s) u(x; z)^2\, dx\right) \tag{2.27}$$

in terms of Painlevé II,[5] namely

$$u_{xx} = 2u^3 + xu, \qquad u(x; z) \simeq \sqrt{z}\, \mathrm{Ai}(x) \quad (x \to \infty). \tag{2.30}$$

2.3.2. *GOE and GSE in the bulk.* With $\sigma(x) = \sigma(x; 1)$ from (2.26) there holds the representation (Basor, Tracy and Widom 1992)

$$E_1(0; s) = \exp\left(-\frac{1}{2}\int_0^{\pi s} \sqrt{\frac{d}{dx} \frac{\sigma(x)}{x}}\, dx\right) E_2(0; s)^{1/2}, \tag{2.31a}$$

$$E_4(0; s/2) = \cosh\left(\frac{1}{2}\int_0^{\pi s} \sqrt{\frac{d}{dx} \frac{\sigma(x)}{x}}\, dx\right) E_2(0; s)^{1/2}. \tag{2.31b}$$

Painlevé representations for $E_1(k; s)$ and $E_4(k; s)$ can be found in Basor et al. (1992).

---

[5]For a better comparison with the other examples we recall that Tracy and Widom (1994a, Eq. (1.16)) also gave the respresentation

$$D_2^{(\text{soft})}(z; (s, \infty)) = \exp\left(-\int_s^\infty \sigma(x; z)\, dx\right) \tag{2.28}$$

in terms of the Jimbo–Miwa–Okamoto σ-form of Painlevé II:

$$\sigma_{xx}^2 = -4\sigma_x(\sigma - x\sigma_x) - 4\sigma_x^3, \qquad \sigma(x; z) \simeq z\left(\mathrm{Ai}'(x)^2 - x\mathrm{Ai}(x)^2\right) \quad (x \to \infty). \tag{2.29}$$

2.3.3. *GOE and GSE at the soft edge.* Tracy and Widom (1996) found, with $u(x) = u(x; 1)$ being the Hastings–McLeod solution of (2.30), the representation

$$F_1(1; s) = \exp\left(-\frac{1}{2}\int_s^\infty u(x)\,dx\right) F_2(1; s)^{1/2}, \qquad (2.32a)$$

$$F_4(1; s) = \cosh\left(\frac{1}{2}\int_s^\infty u(x)\,dx\right) F_2(1; s)^{1/2}. \qquad (2.32b)$$

More general, Dieng (2005) found Painlevé representations of $F_1(k; s)$ and $F_4(k; s)$.

2.4. **Laguerre Ensembles.** Here, we take, on $x \in (0, \infty)$ with parameter $\alpha > -1$, the weight functions[6]

- $w_\alpha(x) = x^\alpha e^{-x/2}$ for $\beta = 1$, the Laguerre Orthogonal Ensemble (LOE),
- $w_\alpha(x) = x^\alpha e^{-x}$ for $\beta = 2$, the Laguerre Unitary Ensemble (LUE),
- $w_\alpha(x) = x^\alpha e^{-x}$ for $\beta = 4$, the Laguerre Symplectic Ensemble (LSE).

We define, for an open interval $J \subset (0, \infty)$, the basic quantity

$$E_{\beta\text{-LE}}^{(n)}(k; J, \alpha) = \mathbb{P}(\text{exactly } k \text{ eigenvalues of the}$$

$$n \times n \text{ Laguerre } \beta\text{-ensemble with parameter } \alpha \text{ lie in } J). \quad (2.33)$$

2.4.1. *Scaling limits.* The large matrix limit at the *hard edge* is (see Forrester 2006, p. 2993)

$$E_\beta^{(\text{hard})}(k; J, \alpha) = \begin{cases} \lim_{n\to\infty} E_{\beta\text{-LE}}^{(n)}(k; 4^{-1}n^{-1}J, \alpha) & \beta = 1 \text{ or } \beta = 2, \\ \lim_{n\to\infty} E_{\beta\text{-LE}}^{(n/2)}(k; 4^{-1}n^{-1}J, \alpha) & \beta = 4. \end{cases} \qquad (2.34)$$

The large matrix limit at the *soft edge* gives exactly the same result (2.4) as for the Gaussian ensembles, namely (see Forrester 2006, p. 2992)

$$E_\beta^{(\text{soft})}(k; J) = \begin{cases} \lim_{n\to\infty} E_{\beta\text{-LE}}^{(n)}(k; 4n + 2(2n)^{1/3}J, \alpha) & \beta = 1 \text{ or } \beta = 2, \\ \lim_{n\to\infty} E_{\beta\text{-LE}}^{(n/2)}(k; 4n + 2(2n)^{1/3}J, \alpha) & \beta = 4, \end{cases} \qquad (2.35)$$

independently of α. Likewise, a proper bulk scaling limit yields $E_\beta^{(\text{bulk})}(k; J)$ as for the Gaussian ensembles (see Tracy and Widom 1994b, p. 291).

In the rest of this section we confine ourselves to the discussion of the LUE; determinantal formulae for LOE and LSE at the hard edge are given in Section 7.

2.5. **Determinantal Representations for the LUE.** Here, the basic formula is (see Mehta 2004, §19.1)

$$E_{\text{LUE}}^{(n)}(k; J, \alpha) = \frac{(-1)^k}{k!} \frac{d^k}{dz^k} D_{\text{LUE}}^{(n)}(z; J, \alpha)\bigg|_{z=1}, \qquad (2.36a)$$

$$D_{\text{LUE}}^{(n)}(z; J, \alpha) = \det\left(1 - z\, K_{n,\alpha}\!\restriction_{L^2(J)}\right), \qquad (2.36b)$$

---

[6]We follow Forrester and Rains (2001) in this particular choice of the weights; as for the Gaussian ensembles notations differ from reference to reference by various scaling factors.

with the Laguerre kernel (the second form follows from Christoffel–Darboux)

$$K_{n,\alpha}(x,y) = \sum_{k=0}^{n-1} \phi_k^{(\alpha)}(x)\phi_k^{(\alpha)}(y) = -\sqrt{n(n+\alpha)} \, \frac{\phi_n^{(\alpha)}(x)\phi_{n-1}^{(\alpha)}(y) - \phi_{n-1}^{(\alpha)}(x)\phi_n^{(\alpha)}(y)}{x-y}$$

(2.37)

that is built from the Laguerre polynomials $L_k^{(\alpha)}(x)$ by the $L^2(0,\infty)$-orthonormal systems of functions

$$\phi_k^{(\alpha)}(x) = \sqrt{\frac{k!}{\Gamma(k+\alpha+1)}} \, x^{\alpha/2} e^{-x/2} L_k^{(\alpha)}(x).$$

(2.38)

The scaling limit at the hard edge is given by (Forrester 1993)

$$E_2^{(\text{hard})}(k; J, \alpha) = \frac{(-1)^k}{k!} \frac{d^k}{dz^k} D_2^{(\text{hard})}(z; J, \alpha)\bigg|_{z=1},$$

(2.39a)

$$D_2^{(\text{hard})}(z; J, \alpha) = \det\left(1 - z\, K_\alpha\!\restriction_{L^2(J)}\right),$$

(2.39b)

with the Bessel kernel

$$K_a(x,y) = \frac{J_\alpha(\sqrt{x})\sqrt{y}\,J_\alpha'(\sqrt{y}) - \sqrt{x}\,J_\alpha'(\sqrt{x})J_\alpha(\sqrt{y})}{2(x-y)}.$$

(2.39c)

Note that for non-integer parameter α the Laguerre kernel $K_{n,\alpha}(x,y)$ and the Bessel kernel $K_\alpha(x,y)$ exhibit algebraic singularities at $x=0$ or $y=0$; see Section A.1 for the bearing of this fact on the choice of numerical methods.

2.6. **Painlevé Representations for the LUE.** Tracy and Widom (1994c) calculated, for the determinant (2.36b) with $J = (0,s)$, the representation

$$D_{\text{LUE}}^{(n)}(z; (0,s), \alpha) = \exp\left(-\int_0^s \frac{\sigma(x;z)}{x}\,dx\right)$$

(2.40)

in terms of the Jimbo–Miwa–Okamoto σ-form of Painlevé V, namely

$$(x\sigma_{xx})^2 = (\sigma - x\sigma_x - 2\sigma_x^2 + (2n+\alpha)\sigma_x)^2 - 4\sigma_x^2(\sigma_x - n)(\sigma_x - n - \alpha),$$

(2.41a)

$$\sigma(x;z) \simeq z\,\frac{\Gamma(n+\alpha+1)}{\Gamma(n)\Gamma(\alpha+1)\Gamma(\alpha+2)} x^{\alpha+1} \qquad (x \to 0).$$

(2.41b)

Accordingly, Tracy and Widom (1994b) obtained, for the determinant (2.39b) of the scaling limit at the hard edge, the representation

$$D_2^{(\text{hard})}(z; (0,s), \alpha) = \exp\left(-\int_0^s \frac{\sigma(x;z)}{x}\,dx\right)$$

(2.42)

in terms of the Jimbo–Miwa–Okamoto σ-form of Painlevé III, namely

$$(x\sigma_{xx})^2 = \alpha^2\sigma_x^2 - \sigma_x(\sigma - x\sigma_x)(4\sigma_x - 1),$$

(2.43a)

$$\sigma(x;z) \simeq \frac{z}{\Gamma(\alpha+1)\Gamma(\alpha+2)}\left(\frac{x}{4}\right)^{\alpha+1} \qquad (x \to 0).$$

(2.43b)

3. Numerics of Painlevé Equations: the Need for Connection Formulae

3.1. **The Straightforward Approach: Solving the Initial Value Problem.** All the five examples (2.24), (2.26), (2.30), (2.41), and (2.43) of a Painlevé representation given in Section 2 take the form of an *asymptotic* initial value problem (IVP); that is, one looks, on a given interval (a, b), for the solution $u(x)$ of a second order ordinary differential equation

$$u''(x) = f(x, u(x), u'(x)) \tag{3.1}$$

subject to an asymptotic "initial" (i.e., one sided) condition, namely *either*

$$u(x) \simeq u_a(x) \qquad (x \to a) \tag{3.2}$$

or

$$u(x) \simeq u_b(x) \qquad (x \to b). \tag{3.3}$$

Although we have given only the first terms of an asymptotic expansion, further terms can be obtained by symbolic calculations. Hence, we can typically *choose* the order of approximation of $u_a(x)$ or $u_b(x)$ at the given "initial" point. Now, the straightforward approach for a numerical solution would be to choose $a_+ > a$ or $b_- < b$ sufficiently close and compute a solution $v(x)$ of the initial value problem

$$v''(x) = f(x, v(x), v'(x)) \tag{3.4}$$

subject to proper initial conditions, namely *either*

$$v(a_+) = u_a(a_+), \qquad v'(a_+) = u_a'(a_+), \tag{3.5}$$

or

$$v(b_-) = u_b(b_-), \qquad v'(b_-) = u_b'(b_-). \tag{3.6}$$

However, for principal reasons that we will discuss in this section, the straightforward IVP approach unavoidably runs into instabilities.

3.1.1. *An example: the Tracy–Widom distribution F_2.* From a numerical point of view, the Painlevé II problem (2.30) is certainly the most extensively studied case. We look at the Hastings–McLeod solution $u(x) = u(x; 1)$ of Painlevé II and the corresponding Tracy–Widom distribution[7]

$$F_2(s) = \exp\left(-\int_s^\infty (x - s)u(x)^2 \, dx\right). \tag{3.7}$$

The initial value problem to be solved numerically is

$$v''(x) = 2v(x)^3 + x\, v(x), \qquad v(b_-) = \mathrm{Ai}(b_-), \quad v'(b_-) = \mathrm{Ai}'(b_-). \tag{3.8}$$

Any value of $b_- \geqslant 8$ gives initial values that are good to machine precision (in IEEE double precision, which is about 16 significant decimal places). We have solved the initial value problem with $b_- = 12$, using a Runge–Kutta method with automatic error and step size control as coded in Matlab's `ode45`, which is essentially the code published in Edelman and Persson (2005) and Edelman and Rao (2005). The red lines in Figure 1 show the absolute error $|v(x) - u(x)|$ and the corresponding error in the calculation of F_2. We observe that the error of $v(x)$

---

[7]There is no need for a numerical quadrature here (and in likewise cases): simply add the differential equation $(\log F_2(s))'' = -u(s)^2$ to the system of differential equations to be solved numerically; see Edelman and Persson (2005). The same idea applies to the BVP approach in Section 3.2.1.

a. error in evaluating $F_2(s)$ b. error in evaluating $u(x)$
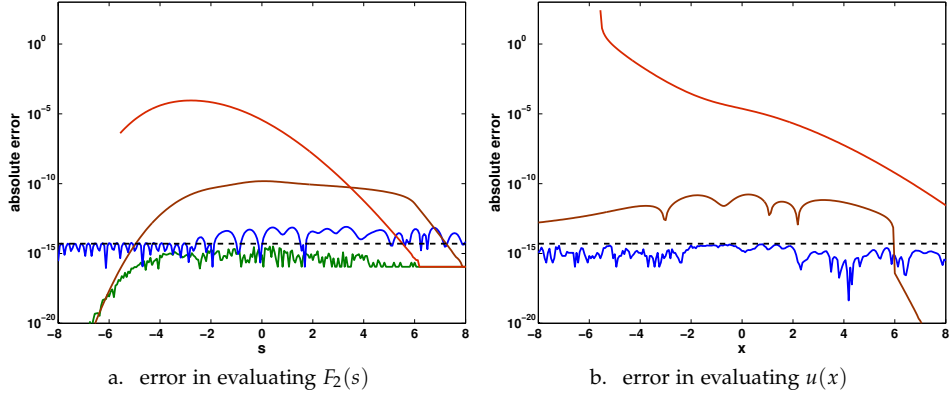
FIGURE 1. Absolute error in evaluating the Tracy–Widom distribution $F_2(s)$ and the Hastings–McLeod solution $u(x)$ of Painlevé II using different numerical methods; red: initial value solution (Matlab's `ode45` as in Edelman and Persson 2005), which breaks down at about $x = -5.56626$; brown: boundary value solution (Matlab's `bvp4c` as in Dieng 2005), blue: boundary value solution by spectral collocation (Driscoll, Bornemann and Trefethen 2008); green: numerical evaluation of the Airy kernel Fredholm determinant (Bornemann 2010a), see also Section 4 (there is no $u(x)$ here). The dashed line shows the tolerance $5 \cdot 10^{-15}$ used in the error control of the last two methods. All calculations were done in IEEE double precision hardware arithmetic.

grows exponentially to the left of b_- and the numerical solution ceases to exist (detecting a singularity) at about $x = -5.56626$. Though the implied values of F_2 are not completely inaccurate, there is a loss of more than 10 digits in absolute precision, which renders the straightforward approach numerically instable (that is, unreliable in fixed precision hardware arithmetic).

To nevertheless obtain a solution that is accurate to 16 digits Prähofer and Spohn (2004) turned, instead of changing the method, to variable precision software arithmetic (using up to 1500 significant digits in Mathematica) and solved the initial value problem with $b_- = 200$ and appropriately many terms of an asymptotic expansion $u_b(x)$. Prähofer (2003) put tables of $u(x)$, $F_2(s)$ and related quantities to the web, for arguments from -40 to 200 with a step size of $1/16$. We have used these data as reference solutions in calculating the errors reported in Figure 1 and Table 1.

3.1.2. *Explaining the instability of the IVP.* By reversibility of the differential equation, finite precision effects in evaluating the initial values at $x = b_-$ can be pulled back to a perturbation of the asymptotic condition $u(x) \simeq \mathrm{Ai}(x)$ for $x \to \infty$. That is, even an *exact* integration of the ordinary differential equation would have to suffer from the result of this perturbation. Let us look at the specific perturbation

$$u(x;\theta) \simeq \theta \cdot \mathrm{Ai}(x) \quad (x \to \infty) \qquad \text{with} \quad \theta = 1 + \epsilon. \tag{3.9}$$

TABLE 1. Maximum absolute error and run time of the methods in Figure 1. The calculation was done for the 401 values of $F_2(s)$ from $s = -13$ to $s = 12$ with step size $1/16$. The IVP solution is only available for the 282 values from $s = -5.5625$ to $s = 12$. All calculations were done in hardware arithmetic.

method	reference	max. error	run time
IVP/Matlab's `ode45`	Edelman and Persson (2005)	$9.0 \cdot 10^{-5}$	11 sec
BVP/Matlab's `bvp4c`	Dieng (2005)	$1.5 \cdot 10^{-10}$	3.7 sec
BVP/spectral colloc.	Driscoll et al. (2008)	$8.1 \cdot 10^{-14}$	1.3 sec
Fredholm determinant	Bornemann (2010a)	$2.0 \cdot 10^{-15}$	0.69 sec

a. $\epsilon = -10^{-8}$ (blue), 0 (green), 10^{-8} (red)   b. $\epsilon = -10^{-16}$ (blue), 0 (green), 10^{-16} (red)
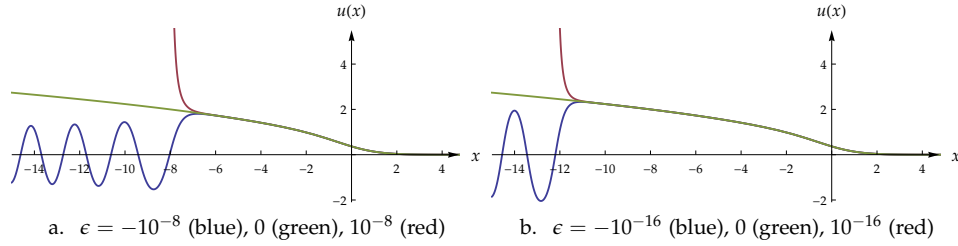
FIGURE 2. Sensitivity of Painlevé II with the asymptotic condition $u(x) \simeq (1 + \epsilon)\,\mathrm{Ai}(x)$ $(x \to \infty)$ for $\epsilon \approx 0$. The calculation was done with variable precision software arithmetic. Observe the dependence of the asymptotic behavior, for $x \to -\infty$, on the sign of ϵ.

The results are shown, for $\epsilon = \pm 10^{-8}$ and $\epsilon = \pm 10^{-16}$ (which is already below the resolution of hardware arithmetic), in Figure 2 (see also Clarkson 2006, Figs. 11/12). Therefore, in hardware arithmetic, an error of order one in computing the Hastings–McLeod solution $u(x) = u(x; 1)$ from the IVP is *unavoidable* already somewhere before $x \approx -12$.

This sensitive behavior can be fully explained by the *connection formulae* of Painlevé II on the real axis, see Clarkson (2006, Thms. 9.1/2) and Fokas, Its, Kapaev and Novokshenov (2006, Thms. 10.1/2). Namely, for the Painlevé II equation (2.30), the given asymptotic behavior $u(x; \theta) \simeq \theta \cdot \mathrm{Ai}(x)$, $\theta > 0$, as $x \to \infty$ implies explicitly known asymptotic behavior "in the direction of $x \to -\infty$":

(1) $0 < \theta < 1$:

$$u(x; \theta) = d(\theta)|x|^{-1/4} \sin\left(\tfrac{2}{3}|x|^{3/2} - \tfrac{3}{4}d(\theta)^2 \log|x| - \phi(\theta)\right)$$
$$+ O(|x|^{-7/10}) \qquad (x \to -\infty), \quad (3.10)$$

with

$$d(\theta)^2 = -\pi^{-1}\log(1 - \theta^2) \tag{3.11a}$$

$$\phi(\theta) = \tfrac{3}{2}d(\theta)^2 \log(2) + \arg\Gamma(1 - \tfrac{i}{2}d(\theta)^2) - \tfrac{\pi}{4}; \tag{3.11b}$$

TABLE 2. Blow-up points $x_0(1 + \epsilon)$ of $u(x; 1 + \epsilon)$ with $\epsilon > 0$.

ϵ	$x_0(1 + \epsilon)$
10^{-4}	$-5.40049\,30292\,23929\cdots$
10^{-8}	$-8.01133\,67804\,74602\cdots$
10^{-12}	$-10.2158\,50522\,53541\cdots$
10^{-16}	$-12.1916\,56643\,75788\cdots$

(2) $\theta = 1$:

$$u(x; 1) = \sqrt{-\frac{x}{2}} + O(x^{-5/2}) \qquad (x \to -\infty); \tag{3.12}$$

(3) $\theta > 1$: there is a pole at a finite $x_0(\theta) \in \mathbb{R}$, such that

$$u(x; \theta) \simeq \frac{1}{x - x_0(\theta)} \qquad (x \downarrow x_0(\theta)). \tag{3.13}$$

We observe that, for $x \to -\infty$, the asymptotic behavior of the Hastings–McLeod solution $u(x; 1)$ *separates* two completely different regimes: an oscillatory ($\theta < 1$) from a blow-up solution ($\theta > 1$). The blow-up points $x_0(\theta)$ are close to the range of values of x which are of interest in the application to RMT, see Table 2.

3.1.3. *Explaining the separation of asymptotic regimes.* The deeper reason for this separation property comes from comparing (2.27) with (2.15b), that is, from the equality

$$\det(I - \theta^2 K_{\mathrm{Ai}}\!\restriction_{L^2(s,\infty)}) = \exp\left(-\int_s^\infty (x - s)u(x; \theta)^2\, dx\right). \tag{3.14}$$

Here, $K_{\mathrm{Ai}}\!\restriction_{L^2(s,\infty)}$ is a positive self-adjoint trace class operator with spectral radius (see Tracy and Widom 1994a)

$$\rho(s) = \lambda_{\max}\left(K_{\mathrm{Ai}}\!\restriction_{L^2(s,\infty)}\right) < 1. \tag{3.15}$$

Obviously, there holds $\rho(s) \to 0$ for $s \to \infty$. On the other hand, since for $\theta = 1$ the determinant (3.14) becomes the Tracy–Widom distribution $F_2(s)$ with $F_2(s) \to 0$ as $s \to -\infty$, we conclude that $\rho(s) \to 1$ as $s \to -\infty$.

Now, we observe that the determinant (3.14) becomes zero if and only if $u(x; \theta)$ blows up at the point $x = s$. By the Painlevé property, such a singularity must be a pole. By Lidskii's theorem (Simon 2005, Thm. 3.7), the determinant (3.14) becomes zero if and only if θ^{-2} is an eigenvalue of $K_{\mathrm{Ai}}\!\restriction_{L^2(s,\infty)}$. Therefore, a blow-up point of $u(x; \theta)$ at $x = s$ implies necessarily that

$$\theta \geqslant \rho(s)^{-1/2} > 1. \tag{3.16}$$

On the other hand, if $\theta > 1$ there must be, by continuity, a largest point $s = x_0(\theta)$ such that $\theta = \rho(s)^{-1/2}$, which gives us the position of the pole of the connection formula. This way, using the methodology of Section 4, we have computed the numbers shown in Table 2.

A similar line of arguments shows that in the other cases (2.24), (2.26), (2.41), and (2.43) of a Painlevé representation given in Section 2, the parameter $z = 1$

(which is the most significant choice for an application to RMT) also belongs to a connecting orbit $\sigma(x;1)$ that separates different asymptotic regimes. In particular, we get poles at finite positions if and only if $z > 1$. Hence, the numerical difficulties observed with the initial value approach have to be expected in general.

3.2. **The Stable Approach: Solving the Boundary Value Problem.** The stable numerical solution of a connecting orbit separating different asymptotic regimes has to be addressed as a two-point *boundary* value problem (BVP), see, e.g., Deuflhard and Bornemann (2002, Chap. 8). That is, we use the information from a connection formula to infer the asymptotic for $x \to b$ from that of $x \to a$, or vice versa, and to approximate $u(x)$ by solving the BVP

$$v''(x) = f(x, v(x), v'(x)), \qquad v(a_+) = u_a(a_+), \quad v(b_-) = u_b(b_-). \qquad (3.17)$$

Thus, four particular choices have to be made: The values of the finite boundary points a_+ and b_-, and the truncation indices of the asymptotic expansions at $x \to a$ and $x \to b$ that give the boundary functions $u_a(x)$ and $u_b(x)$. All this has to be balanced for the accuracy and efficiency of the final method.[8]

3.2.1. *An Example: the Tracy–Widom distribution $F_2(x)$.* Let us look, once more, at the Hastings–McLeod solution $u(x) = u(x;1)$ of (2.30) and the corresponding Tracy–Widom distribution (3.7). By definition, we have

$$u(x) \simeq \mathrm{Ai}(x) \qquad (x \to \infty). \qquad (3.18)$$

The asymptotic result for $x \to -\infty$ as given in the connection formula (3.12) is not accurate enough to allow a sufficiently large point a_+ to be used. However, using symbolic calculations it is straightforward to obtain, from this seed, the asymptotic expansion (Tracy and Widom 1994a, Eq. (4.1))

$$u(x) = \sqrt{-\frac{x}{2}} \left(1 + \frac{1}{8}x^{-3} - \frac{73}{128}x^{-6} + \frac{10657}{1024}x^{-9} - \frac{13912277}{32768}x^{-12} + O(x^{-15}) \right)$$
$$(x \to -\infty). \quad (3.19)$$

Dieng (2005) chooses these terms as $u_a(x)$, as well as $a_+ = -10$, $b_- = 6$ and $u_b(x) = \mathrm{Ai}(x)$. Using Matlab's fixed-order collocation method `bvp4c`, he calculates solutions whose errors are assessed in Figure 1 and Table 1. The accuracy is still somewhat limited and he reports (p. 88) on difficulties in obtaining a starting iterate for the underlying nonlinear solver. A more promising and efficient approach to obtain near machine precision is the use of spectral collocation methods. Because of analyticity, the convergence will be exponentially fast. This can be most elegantly expressed in the newly developed `chebop` system of Driscoll et al. (2008), a Matlab extension for the automatic solution of differential equations by spectral collocation. In fact, the evaluation of the Tracy–Widom distribution is Example 6.2 in that paper. Here, the first four terms of (3.19) are chosen as $u_a(x)$, as well as $a_+ = -30$, $b_- = 8$

---

[8]An early variant of this connection-formula based approach can be traced back to the work of Wu, McCoy, Tracy and Barouch (1976, App. A): there, a Painlevé III representation of the spin-spin correlation function of the two-dimensional Ising model was evaluated by joining a forward integration of the IVP from a_+ to some interior point $c \in (a_+, b_-)$ with a backward integration of the IVP from b_- to c. The difference of the two IVP solutions at c was used as a rough error estimate. Though not quite a BVP solution, it is close in spirit. Actually, this was the approach originally used by Tracy and Widom (1993b, 1994a) in their numerical evaluation of F_2 (personal communication by Craig Tracy).

and $u_b(x) = \text{Ai}(x)$. The Newton iteration is started from a simple affine function satisfying the boundary conditions; see Figure 1 and Table 1 for a comparison of the accuracy and run time.

3.3. **A List of Connection Formulae.** For the sake of completeness we collect the connection formulae for the other Painlevé representations (2.24), (2.26), (2.41), and (2.43). References are given to the place where we have found each formula; we did not try to locate the historically first source, whatsoever. Note that a rigorous derivation of a connection formula relies on deep and involved analytic arguments and calculations; a systematic approach is based on Riemann–Hilbert problems, see Deift (1999b) and Fokas et al. (2006) for worked out examples.

- The Painlevé III representation (2.43), for LUE with parameter α at the hard edge, satisfies (Tracy and Widom 1994b, Eq. (3.1))

$$\sigma(x;1) = \frac{x}{4} - \frac{\alpha}{2}\sqrt{x} + O(1) \qquad (x \to \infty). \tag{3.20}$$

- The Painlevé IV representation (2.24), for n-dimensional GUE, satisfies (Tracy and Widom 1994c, Eq. (5.17))

$$\sigma(x;1) = -2nx - nx^{-1} + O(x^{-3}) \qquad (x \to -\infty). \tag{3.21}$$

  It is mentioned there that $\sigma(x;z)$ has, for $z > 1$, poles at finite positions. This is consistent with the line of arguments that we gave in Section 3.1.3.

- The Painlevé V representation (2.26), for the bulk scaling limit of GUE, satisfies (Basor et al. 1992, p. 6)

$$\sigma(x;z) \simeq \begin{cases} \dfrac{x^2}{4} & z = 1 \\ -\log(1-z)\dfrac{x}{\pi} & 0 < z < 1 \end{cases} \qquad (x \to \infty) \tag{3.22}$$

- The Painlevé V representation (2.41), for n-dimensional LUE with parameter α, satisfies (Forrester and Witte 2002, Eq. (1.42))

$$\sigma(x;1) = nx - \alpha n + \alpha n^2 x^{-1} + O(x^{-2}) \qquad (x \to \infty). \tag{3.23}$$

3.4. **Summary.** Let us summarize the steps that are necessary for the numerical evaluation of a distribution function from RMT given by a Painlevé representation on the interval (a, b) (that is, the second order differential equation is given together with an asymptotic expansion of its solution at just *one* of the endpoints a or b):

(1) Derive (or locate) the corresponding connection formula that gives the asymptotic expansion at the other end point. This requires considerable analytic skills or, at least, a broad knowledge of the literature.

(2) Choose $a_+ > a$ and $b_- < b$ together with indices of truncation of the asymptotic expansions such that the expansions themselves are sufficiently accurate in (a, a_+) and (b_-, b) and the two-point boundary value problem (3.17) can be solved efficiently. This balancing of parameters requires a considerable amount of experimentation to be successful.

(3) The issues of solving the boundary value problem (3.17) have to be addressed: starting values for the Newton iteration, the discretization of the differential equation, automatic step size control etc. This requires a considerable amount of experience in numerical analysis.

Thus, much work has still to be done to make all this a "black-box" approach.

4. Numerics of Fredholm Determinants and Their Derivatives

4.1. **The Basic Method.** Bornemann (2010a) has recently shown that there is an extremely simple, accurate, and general direct numerical method for evaluating Fredholm determinants. By taking an m-point quadrature rule[9] of order[10] m with nodes $x_j \in (a, b)$ and *positive* weights w_j, written in the form

$$\sum_{j=1}^{m} w_j f(x_j) \approx \int_a^b f(x)\, dx, \tag{4.1}$$

the Fredholm determinant

$$d(z) = \det(I - zK\!\restriction_{L^2(a,b)}) \tag{4.2}$$

is simply approximated by the corresponding m-dimensional determinant

$$d_m(z) = \det\left(\delta_{ij} - z\, w_i^{1/2} K(x_i, x_j) w_j^{1/2}\right)_{i,j=1}^{m}. \tag{4.3}$$

This algorithm can straightforwardly be implemented in a few lines. It just needs to call the kernel $K(x, y)$ for evaluation and has only one method parameter, the approximation dimension m.

If the kernel function $K(x, y)$ is analytic in a complex neighborhood of (a, b), one can prove exponential convergence (Bornemann 2010a, Thm. 6.2): there is a constant $\rho > 1$ (depending on the domain of analyticity of K) such that

$$d_m(z) - d(z) = O(\rho^{-m}) \qquad (m \to \infty), \tag{4.4}$$

locally uniform in $z \in \mathbb{C}$. (Note that $d(z)$ is an *entire* function and $d_m(z)$ a polynomial.) This means, in practice, that doubling m will double the number of correct digits; machine precision of about 16 digits is then typically obtained for a relatively small dimension m between 10 and 100. This way the evaluation of the Tracy–Widom distribution $F_2(s)$, at a given argument s, takes just a few milliseconds; see Figure 1 and Table 1 for a comparison of the accuracy and run time with the evaluation of the Painlevé representation.

4.2. **Numerical Evaluation of Finite-Dimensional Determinants.** Let us write

$$d_m(z) = \det(I - zA_m), \qquad A_m \in \mathbb{R}^{m \times m}, \tag{4.5}$$

for the finite-dimensional determinant (4.3). Depending on whether we need its value for just one z (typically $z = 1$ in the context of RMT) or for several values of z (such as for the calculation of derivatives), we actually proceed as follows:

(1) The *value* $d_m(z)$ at a given point $z \in \mathbb{C}$ is calculated from the *LU* decomposition of the matrix $I - zA_m$ (with partial pivoting). Modulo the proper sign (obtained from the pivoting sequence), the value is given by the product of the diagonal entries of U (Stewart 1998, p. 176). The computational cost is of order $O(m^3)$, including the cost for obtaining the weights and nodes of the quadrature method, see Bornemann (2010a, Footnote 5).

---

[9]We choose Clenshaw–Curtis quadrature, with a suitable meromorphic transformation for (semi) infinite intervals (Bornemann 2010a, Eq. (7.5)). For the use of Gauss–Jacobi quadrature see Section A.1.

[10]A quadrature rule is of order m if it is *exact* for polynomials of degree $m - 1$.

(2) The polynomial function $d_m(z)$ itself is represented by

$$d_m(z) = \prod_{j=1}^{m}(1 - z\lambda_j(A_m)). \tag{4.6}$$

Here, we first calculate the eigenvalues $\lambda_j(A_m)$ (which is slightly more expensive than the *LU* decomposition, although the computational cost of, e.g., the *QR* algorithm is of order $O(m^3)$, too). The subsequent evaluation of $d_m(z)$ costs just $O(m)$ operations for each point z that we care to address.

4.3. **Numerical Evaluation of Higher Derivatives.** The numerical evaluation of expressions such as (2.11a) requires the computation of derivatives of the determinant $d(z)$ with respect to z. We observe that, by well known results from complex analysis, these derivatives enjoy the same kind of convergence as in (4.4),

$$d_m^{(k)}(z) - d^{(k)}(z) = O(\rho^{-m}) \qquad (m \to \infty), \tag{4.7}$$

locally uniform in $z \in \mathbb{C}$, with an arbitrary but fixed $k = 0, 1, 2, \dots$

The numerical evaluation of higher derivatives is, in general, a badly conditioned problem. However, for *entire* functions f such as our determinants we can make use of the Cauchy integrals[11]

$$f^{(k)}(z) = \frac{k!}{2\pi r^k} \int_0^{2\pi} e^{-ik\theta} f(z + re^{i\theta})\, d\theta \qquad (r > 0). \tag{4.8}$$

Since the integrand is analytic and *periodic*, the simple trapezoidal rule is exponentially convergent (Davis and Rabinowitz 1984, §4.6.5); that is, once again, p quadrature points give an error $O(\rho^{-p})$ for some constant $\rho > 1$.

Theoretically, all radii $r > 0$ are equivalent. Numerically, one has to be very careful in choosing a proper radius r (for a detailed study see Bornemann 2009). The quantity of interest in controlling this choice is the condition number of the integral, that is, the ratio

$$\kappa = \left| \int_0^{2\pi} e^{-ik\theta} f(z + re^{i\theta})\, d\theta \right| \bigg/ \int_0^{2\pi} |f(z + re^{i\theta})|\, d\theta. \tag{4.9}$$

For reasons of numerical stability, we should choose r such that $\kappa \approx 1$. Some experimentation has led us to the choices $r = 1$ for the bulk and $r = 0.1$ for the edge scaling limits (but see also Example 12.3 in Bornemann 2009).

4.4. **Error Control.** Exponentially convergent sequences allow us to control the error of approximation in a very simple fashion. Let us consider a sequence $d_m \to d$ with the convergence estimate

$$d_m - d = O(\rho^{-m}) \tag{4.10}$$

for some constant $\rho > 1$. If the estimate is sharp, it implies the quadratic convergence of the contracted sequence d_{2^q}, namely

$$|d_{2^{q+1}} - d| \leqslant c|d_{2^q} - d|^2 \tag{4.11}$$

---

[11]For more general analytic f one would have to bound the size of the radius r to not leave the domain of analyticity. In particular, when evaluating (2.16) we have to take care of the condition $r < \min |(1 - \lambda)/\lambda|$, where λ runs through the eigenvalues of the matrix kernel operator.

TABLE 3. Approximation of the Airy kernel determinant $F_2(-2) = \det(I - K_{\mathrm{Ai}}\restriction_{L^2(-2,\infty)})$ by (4.3), using m-point Clenshaw–Curtis quadrature meromorphically transformed to the interval $(-2,\infty)$, see Bornemann (2010a, Eq. (7.5)). Observe the apparent quadratic convergence: the number of correct digits doubles from step to step. Thus, in exact arithmetic, the value for $m = 64$ would be correct to about 20 digits; here, the error saturates at the level of machine precision ($2.22 \cdot 10^{-16}$): all 15 digits shown for the $m = 64$ approximation are correct.

m	d_m	$|d_m - F_2(-2)|$	error estimate (4.12)
8	0.38643 72955 15158	$2.67868 \cdot 10^{-2}$	$2.67817 \cdot 10^{-2}$
16	0.41321 90011 46910	$5.14136 \cdot 10^{-6}$	$5.14138 \cdot 10^{-6}$
32	0.41322 41425 27728	$2.26050 \cdot 10^{-11}$	$2.26046 \cdot 10^{-11}$
64	0.41322 41425 05123	$4.44089 \cdot 10^{-16}$	—

for some $c > 0$. A simple application of the triangle inequality gives then

$$|d_{2^q} - d| \leqslant \frac{|d_{2^q} - d_{2^{q+1}}|}{1 - c|d_{2^q} - d|} \simeq |d_{2^q} - d_{2^{q+1}}| \qquad (q \to \infty). \qquad (4.12)$$

Thus we take $|d_{2^q} - d_{2^{q+1}}|$ as an excellent error estimate of $|d_{2^q} - d|$ and as a quite "conservative" but absolutely reliable estimate of $|d_{2^{q+1}} - d|$. Table 3 exemplifies this strategy for the calculation of the value $F_2(-2)$.

4.5. **Numerical Evaluation of Densities.** The numerical evaluation of the probability densities belonging to the cumulative distribution functions $F(s)$ given by a determinantal expression requires a low order differentiation with respect to the *real-valued* variable s (which cannot easily be extended *numerically* into the complex domain). Nevertheless these functions are typically real-analytic and therefore amenable to an excellent approximation by interpolation in Chebyshev points. To be specific, if $F(s)$ is given on the finite interval $[a, b]$ and $s_0, \ldots, s_m$ denote the Chebyshev points of that interval, the polynomial interpolant $p_m(s)$ of degree m is given by Salzer's (1972) barycentric formula

$$p_m(s) = \frac{\sum_{k=0}^{\prime\prime m} (-1)^k F(s_k) / (s - s_k)}{\sum_{k=0}^{\prime\prime m} (-1)^k / (s - s_k)}, \qquad (4.13)$$

where the double primes denote trapezoidal sums, i.e., the first and last term of the sums get a weight $1/2$. This formula enjoys perfect numerical stability (Higham 2004). If F is real analytic, we have exponential convergence once more, that is

$$\|F - p_m\|_\infty = O(\rho^{-m}) \qquad (m \to \infty) \qquad (4.14)$$

for some constant $\rho > 1$ (see Berrut and Trefethen 2004). Low order derivatives (such as densities) and integrals (such as moments) can easily be calculated from this interpolant. All that is most conveniently implemented in Battles and Trefethen's (2004) chebfun package for Matlab (see also Driscoll et al. 2008).
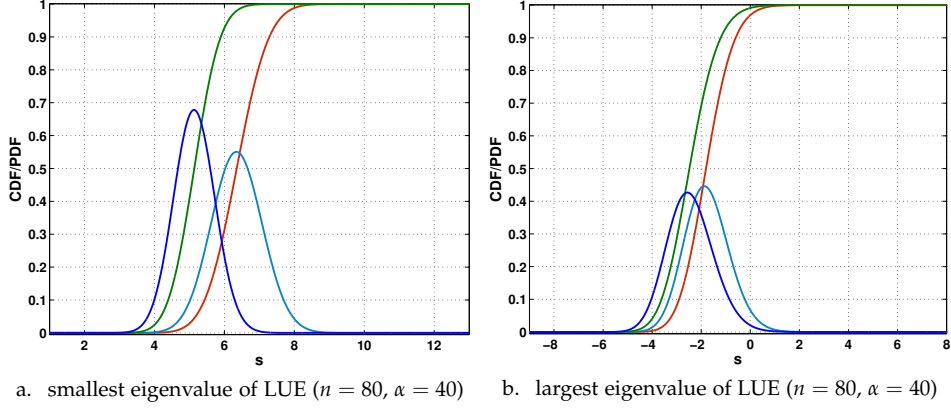
a. smallest eigenvalue of LUE ($n = 80$, $\alpha = 40$)   b. largest eigenvalue of LUE ($n = 80$, $\alpha = 40$)

FIGURE 3. CDF (green) and PDF (dark blue) of the smallest and largest eigenvalue for n-dimensional LUE with parameter α with $n = 80$, $\alpha = 40$. Also shown are the scaling limits at the hard and soft edge (CDF in red, PDF in light blue).

4.6. **Examples.** We illustrate the method with three examples. More about the software that we have written can be found in Section 9.

4.6.1. *Distribution of smallest and largest level in a specific LUE.* We evaluate the cumulative distribution functions (CDF) and probability density functions (PDF) of the smallest and largest eigenvalue of the n-dimensional LUE with parameter α for the specific choices $n = 80$ and $\alpha = 40$. (Note that for parameters of this size the numerical evaluation of the Painlevé representation (2.41) becomes extremely challenging.) Specifically, we evaluate the CDFs (the PDFs are their derivatives)

$$\mathbb{P}(\lambda_{\min} \leqslant s) = 1 - E_{\text{LUE}}^{(n)}(0; (0, s), \alpha) \tag{4.15}$$

and

$$\mathbb{P}(\lambda_{\max} \leqslant 4n + 2\alpha + 2 + 2(2n)^{1/3}s)$$
$$= E_{\text{LUE}}^{(n)}(0; (4n + 2\alpha + 2 + 2(2n)^{1/3}s, \infty), \alpha). \tag{4.16}$$

Additionally, we calculate the CDFs of the scaling limits; that is,

$$1 - E_2^{(\text{hard})}(0; (0, 4ns), \alpha) \tag{4.17}$$

at the hard edge and the Tracy–Widom distribution

$$F_2(s) = E_2^{(\text{soft})}(0; (s, \infty)) \tag{4.18}$$

at the soft edge. All that has to be done to apply our method is to simply code the Laguerre, Bessel, and Airy kernels. Figure 3 visualizes the functions and Table 4 shows their moments to 10 correct decimal places.

TABLE 4. Moments of the distributions (4.15), (4.16), (4.17), and (4.18) for LUE with $n = 80$ and $\alpha = 40$. We show ten correctly *truncated* digits (that passed the error control) and give the computing time. All calculations were done in hardware arithmetic.

CFD	mean	variance	skewness	kurtosis	time
(4.15)	5.14156 81318	0.34347 52478	0.04313 30951	−0.02925 63564	1.0 sec
(4.17)	6.35586 98372	0.52106 15307	0.04102 67718	−0.02943 22640	1.2 sec
(4.16)	−2.43913 84563	0.89341 23428	0.26271 64962	0.12783 51672	4.1 sec
(4.18)	−1.77108 68074	0.81319 47928	0.22408 42036	0.09344 80876	1.0 sec

a. k-level spacing functions $E_2(k; s)$ of GUE   b. density $\partial_s F_2(k; s)$ of k-th largest level in GUE
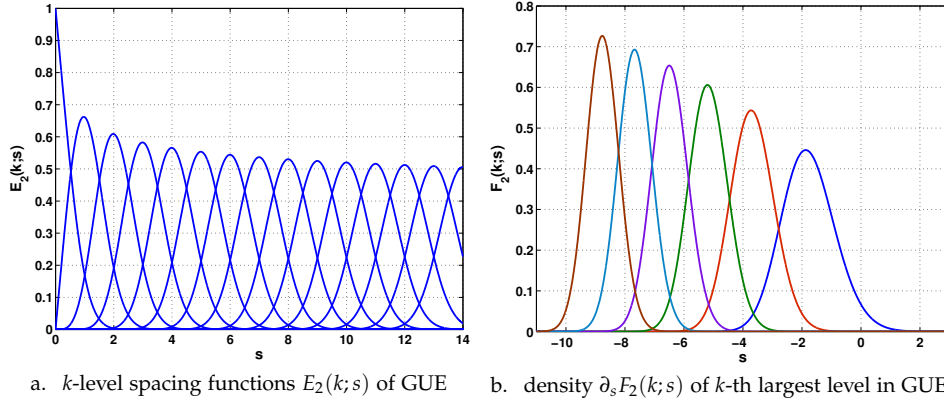
FIGURE 4. Plots of the k-level spacing functions $E_2(k; s)$ in the bulk scaling limit of GUE ($k = 0, \ldots, 14$; larger k go to the right), and of the probability density functions $\partial_s F_2(k; s)$ of the k-th largest level in the soft edge scaling limit of GUE ($k = 1, \ldots, 6$; larger k go to the left). The underlying calculations were all done in hardware arithmetic and are accurate to an absolute error of about $5 \cdot 10^{-15}$. Each of the two plots took a run time of about 30 seconds. Compare with Mehta (2004, Fig. 6.4) and Tracy and Widom (1994a, Fig. 2).

4.6.2. *The distribution of k-level spacings in the bulk of GUE.* By (2.5) and (2.14), the k-level spacing functions in the bulk scaling limit of GUE are given by the determinantal expressions

$$E_2(k; s) = \frac{(-1)^k}{k!} \frac{d^k}{dz^k} \det \left(I - z K_{\sin} \upharpoonright_{L^2(0,s)} \right) \Bigg|_{z=1}. \qquad (4.19)$$

Mehta and des Cloizeaux (1972) evaluated them using Gaudin's method (which be briefly described in Section 1.1.1); a plot of these functions, for k from 0 up to 14, can also be found in Mehta (2004, Fig. 6.4). Now, the numerical evaluation of the expression (4.19) is directly amenable to our approach. The results of our calculations are shown in Figure 4.a.

4.6.3. *The distributions of the k-th largest level at the soft edge of GUE.* By (2.9) and (2.15), the cumulative distribution functions of the k-th largest level in the soft edge scaling limit of GUE are given by the determinantal expressions

$$F_2(k;s) = \sum_{j=0}^{k-1} \frac{(-1)^j}{j!} \frac{d^j}{dz^j} \det\left(I - z\, K_{\mathrm{Ai}}\!\restriction_{L^2(s,\infty)}\right)\Big|_{z=1}, \tag{4.20}$$

which is directly amenable to be evaluated by our numerical approach. The results of our calculations are shown in Figure 4.b.

Remark. To our knowledge, prior to this work, only calculations of the particular cases $k = 1$ (the largest level) and $k = 2$ (the next-largest level) have been reported in the literature (Tracy and Widom 2000, Dieng 2005). These calculations were based on the representation (2.27) of the determinant in terms of the Painlevé II equation (2.30). The evaluation of $F_2(s) = F_2(1;s)$ was obtained from the Hastings–McLeod solution $u(x) = u(x;1)$, see Section 3.2.1. On the other hand, the evaluation of $F_2(2;s)$ required the function

$$w(x) = \partial_z u(x;z)|_{z=1}, \tag{4.21}$$

which, by differentiating (2.30), is easily seen to satisfy the linear ordinary differential equation

$$w''(x) = (6u(x)^2 + x)w(x), \qquad w(x) \simeq \tfrac{1}{2}\mathrm{Ai}(x) \quad (x \to \infty). \tag{4.22}$$

Obtaining the analogue of the connection formula (3.19) requires some work (though, since the underlying differential equation is linear, it poses no fundamental difficulty) and one gets (see Tracy and Widom (1994a, p. 164) who also give expansions for larger k)

$$w(x) = \frac{e^{2\sqrt{2}(-x)^{3/2}/3}}{2^{7/4}\sqrt{\pi}(-x)^{1/4}} \left(1 + \frac{17}{48\sqrt{2}}(-x)^{-3/2} - \frac{1513}{9216}x^{-3} + O((-x)^{-9/2})\right)$$
$$(x \to -\infty). \tag{4.23}$$

Note that the exponential growth points, once more, to the instability we have discussed in Section 3.1.2.

5. The Distribution of k-Level Spacings in the Bulk: GOE and GSE

Mehta (2004, Chap. 20) gives determinantal formulae for the k-level spacing functions $E_\beta(k;s)$ in the bulk scaling limit that are (also in the cases $\beta = 1$ and $\beta = 4$ of the GOE and GSE, respectively) directly amenable to the numerical approach of Section 4. These formulae are based on a factorization of the sine kernel determinant (2.14b), which we describe first.

Since $K_{\sin}$ is a convolution operator we have the shift invariance

$$\det\left(I - zK_{\sin}\!\restriction_{L^2(0,2t)}\right) = \det\left(I - zK_{\sin}\!\restriction_{L^2(-t,t)}\right). \tag{5.1}$$

Next, there is the orthogonal decomposition $L^2(-t,t) = X_t^{\mathrm{even}} \oplus X_t^{\mathrm{odd}}$ into the even and odd functions. On the level of operators, this corresponds to the block

diagonalization

$$K_{\sin}\!\restriction_{L^2(-t,t)} = \begin{pmatrix} K_{\sin}^+ & \\ & K_{\sin}^- \end{pmatrix} \restriction_{X_t^{\text{even}} \oplus X_t^{\text{odd}}} \tag{5.2}$$

with the kernels

$$K_{\sin}^\pm(x,y) = \tfrac{1}{2}(K_{\sin}(x,y) \pm K_{\sin}(x,-y)). \tag{5.3}$$

Further, there is obviously

$$K_{\sin}^+\!\restriction_{L^2(-t,t)} = \begin{pmatrix} K_{\sin}^+ & \\ & 0 \end{pmatrix} \restriction_{X_t^{\text{even}} \oplus X_t^{\text{odd}}}, \qquad K_{\sin}^-\!\restriction_{L^2(-t,t)} = \begin{pmatrix} 0 & \\ & K_{\sin}^- \end{pmatrix} \restriction_{X_t^{\text{even}} \oplus X_t^{\text{odd}}}. \tag{5.4}$$

Hence, we get the factorization

$$\det\left(I - zK_{\sin}\!\restriction_{L^2(-t,t)}\right) = \det\left(I - zK_{\sin}^+\!\restriction_{L^2(-t,t)}\right)\det\left(I - zK_{\sin}^-\!\restriction_{L^2(-t,t)}\right). \tag{5.5}$$

Now, upon introducing the functions

$$E_\pm(k;s) = \frac{(-1)^k}{k!}\frac{d^k}{dz^k}\det\left(I - z\,K_{\sin}^\pm\!\restriction_{L^2(-s/2,s/2)}\right)\Bigg|_{z=1} \tag{5.6}$$

we obtain, using the factorization (5.5) and the Leibniz formula applied to (4.19), the representation

$$E_2(k;s) = \sum_{j=0}^{k} E_+(j;s)E_-(k-j;s) \tag{5.7}$$

of the k-level spacing functions in the bulk of GUE. The important point here is that Mehta (2004, Eqs. (20.1.20/21)) succeeded in representing the k-level spacing functions of GOE and GSE in terms of the functions $E_\pm$, too:

$$E_1(0;s) = E_+(0;s), \tag{5.8a}$$

$$E_1(2k-1;s) = E_-(k-1;s) - E_1(2k-2;s), \tag{5.8b}$$

$$E_1(2k;s) = E_+(k;s) - E_1(2k-1;s), \tag{5.8c}$$

$(k = 1,2,3,\ldots)$ for GOE and

$$E_4(k;s) = \tfrac{1}{2}(E_+(k;2s) + E_-(k;2s)) \tag{5.9}$$

$(k = 0,2,3,\ldots)$ for GSE. Based on these formulae, we have used the numerical methods of Section 4 to reproduce the plots of Mehta (2004, Figs. 7.3/11.1). The results of our calculations are shown in Figure 5.

6. The k-th Largest Level at the Soft Edge: GOE and GSE

In this section we derive new determinantal formulae for the cumulative distribution functions $F_1(k;s)$ and $F_4(k;s)$ of the k-th largest level in the soft edge scaling limit of GOE and GSE. We recall from (2.9) that

$$F_\beta(k;s) = \sum_{j=0}^{k-1} \tilde{E}_\beta(j;s), \tag{6.1}$$

where we briefly write

$$\tilde{E}_\beta(k;s) = E_\beta^{(\text{soft})}(k;(s,\infty)). \tag{6.2}$$

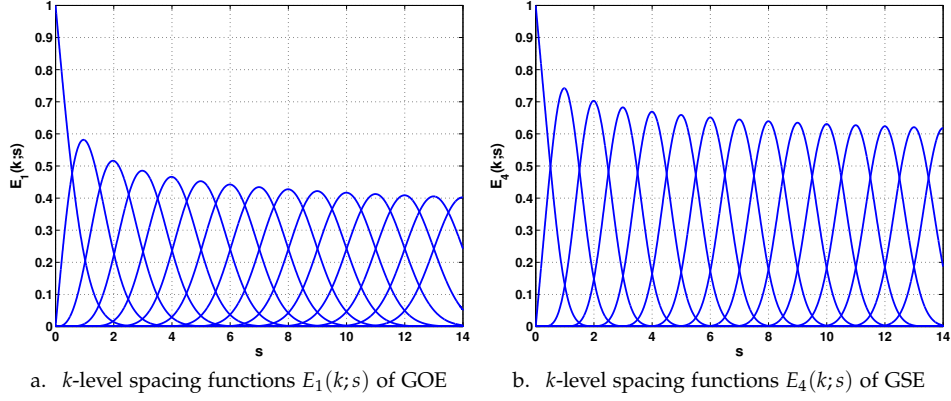a. *k*-level spacing functions $E_1(k;s)$ of GOE   b. *k*-level spacing functions $E_4(k;s)$ of GSE

FIGURE 5. Plots of the *k*-level spacing functions $E_1(k;s)$ in the bulk scaling limit of GOE and $E_4(k;s)$ in the bulk scaling limit of GSE ($k = 0,\dots,14$; larger *k* go to the right). The underlying calculations were all done in hardware arithmetic and are accurate to an absolute error of about $5 \cdot 10^{-15}$. Each of the two plots took a run time of less than one minute. Compare with Mehta (2004, Figs. 7.3/11.1).

The new determinantal formulae of this section are amenable to the efficient numerical evaluation by the methods of Section 4; but, more important, they are derived from a determinantal equation (6.10) whose truth we established by numerical experiments *before* proving it rigorously. Therefore, we understand this section as an invitation to the area of Experimental Mathematics (Borwein and Bailey 2004).

In a broad analogy to the previous section we start with a factorization of the Airy kernel determinant (2.15b) that we have learnt from Ferrari and Spohn (2005, Eq. (34)). Namely, the integral representation

$$K_{\mathrm{Ai}}(x,y) = \int_0^\infty \mathrm{Ai}(x + \xi)\mathrm{Ai}(y + \xi)\, d\xi \tag{6.3}$$

of the Airy kernel implies, by introducing the kernels

$$T_s(x,y) = \mathrm{Ai}(x + y + s), \qquad V_{\mathrm{Ai}}(x,y) = \frac{1}{2}\mathrm{Ai}\left(\frac{x+y}{2}\right), \tag{6.4}$$

the factorization

$$\det\left(I - zK_{\mathrm{Ai}}\restriction_{L^2(s,\infty)}\right) = \det\left(I - z\left(T_s\restriction_{L^2(0,\infty)}\right)^2\right)$$

$$= \det\left(I - \sqrt{z}\, T_s\restriction_{L^2(0,\infty)}\right)\cdot\det\left(I + \sqrt{z}\, T_s\restriction_{L^2(0,\infty)}\right)$$

$$= \det\left(I - \sqrt{z}\, V_{\mathrm{Ai}}\restriction_{L^2(s,\infty)}\right)\cdot\det\left(I + \sqrt{z}\, V_{\mathrm{Ai}}\restriction_{L^2(s,\infty)}\right) \tag{6.5}$$

that is valid for the complex cut plane $z \in \mathbb{C} \setminus (-\infty, 0]$. Now, upon introducing the functions

$$\tilde{E}_{\pm}(k; s) = \left. \frac{(-1)^k}{k!} \frac{d^k}{dz^k} \det \left(I \mp \sqrt{z} \, V_{\text{Ai}} \!\restriction_{L^2(s,\infty)} \right) \right|_{z=1} \tag{6.6}$$

we obtain, using the factorization (6.5) and the Leibniz formula applied to (2.15), the representation

$$\tilde{E}_2(k; s) = \sum_{j=0}^{k} \tilde{E}_+(j; s) \tilde{E}_-(k - j; s). \tag{6.7}$$

Further, Ferrari and Spohn (2005, Eqs. (33/35)) proved that

$$\tilde{E}_1(0; s) = \tilde{E}_+(0; s) \tag{6.8a}$$

$$\tilde{E}_4(0; s) = \tfrac{1}{2}(\tilde{E}_+(0; s) + \tilde{E}_-(0; s)). \tag{6.8b}$$

The similarity of the pairs of formulae (6.7)/(5.7), (6.8a)/(5.8a), and (6.8b)/(5.9) (the last with $k = 0$) is absolutely striking. So we asked ourselves whether (6.8b) generalizes to the analogue of (5.9) for general k, that is, whether

$$\tilde{E}_4(k; s) = \tfrac{1}{2}(\tilde{E}_+(k; s) + \tilde{E}_-(k; s)) \qquad (k = 0, 1, 2, \ldots) \tag{6.9}$$

is valid in general. In view of (2.16) such a result is *equivalent* to the following theorem. We first convinced ourselves of its truth in the sense of experimental mathematics: by numerically[12] checking its assertion for 100 000 randomly chosen arguments. Thus being encouraged, we then worked out the proof given below.[13]

Theorem 6.1. *The determinantal equation*

$$D_4(z; (s, \infty))^{1/2}$$

$$= \frac{1}{2} \left(\det \left(I - \sqrt{z} \, V_{\text{Ai}} \!\restriction_{L^2(s,\infty)} \right) + \det \left(I + \sqrt{z} \, V_{\text{Ai}} \!\restriction_{L^2(s,\infty)} \right) \right) \tag{6.10}$$

holds for all $s \in \mathbb{R}$ and z in the complex domain of analyticity that contains $z = 1$.

Proof. Since the operator theoretic arguments of Ferrari and Spohn (2005) cannot directly be extended to yield (6.10) we proceed by using Painlevé representations. Dieng (2005, Thm. 1.2.1, Eq. (1.2.2)) proved that (2.32b) generalizes to

$$D_4(\theta^2; (s, \infty))^{1/2} = D_2^{(\text{soft})}(\theta^2; (s, \infty))^{1/2} \cosh \left(\frac{1}{2} \int_s^{\infty} u(x; \theta) \, dx \right) \tag{6.11a}$$

in terms of the Painlevé representation

$$u_{xx} = 2u^3 + xu, \qquad u(x; \theta) \simeq \theta \cdot \text{Ai}(x) \quad (x \to \infty). \tag{6.11b}$$

Here we put $\sqrt{z} = \theta$ and observe that (6.11a) obviously extends, by the symmetry of the Painlevé II equation, from $0 < \theta \leqslant 1$ to the range $-1 \leqslant \theta \leqslant 1$. In view

---

[12]The function $D_4(z; (s, \infty))$ was evaluated using the extension of our method to matrix kernel determinants that will be discussed in Section 8.1; see also Example 9.2.2 for a concrete instance.

[13]Later though, we found that the result has recently been established by Forrester (2006, Eq. (1.23)).

of (2.28) Dieng's representation (6.11a) readily implies, by analytic continuation, the asserted formula (6.10) *if* the representation

$$\det\left(I - \theta\, V_{\mathrm{Ai}}\!\restriction_{L^2(s,\infty)}\right) = \exp\left(-\frac{1}{2}\int_s^\infty u(x;\theta)\,dx\right)\det\left(I - \theta^2\,K_{\mathrm{Ai}}\!\restriction_{L^2(s,\infty)}\right)^{1/2}$$

$$= \exp\left(-\frac{1}{2}\int_s^\infty \left(u(x;\theta) + (x-s)u(x;\theta)^2\right)dx\right) \quad (6.12)$$

happens to be true for all $-1 \leqslant \theta \leqslant 1$ (note that we have chosen the signs in accordance with the the special cases $\theta = \pm 1$ as given by (6.8) and (2.32)). Now, this particular Painlevé representation can directly be read off from the work of Desrosiers and Forrester (2006, Eqs. (4.8/19)), which completes the proof. $\square$

It remains to establish formulae for the GOE functions $\tilde{E}_1(k;s)$ that are structurally similar to (5.8). To this end we use the interrelationships between GOE, GUE, and GSE found by Forrester and Rains (2001, Thm. 5.2),[14] which can symbolically be written in the form

$$\mathrm{GSE}_n = \mathrm{even}(\mathrm{GOE}_{2n+1}), \qquad\qquad\qquad (6.13a)$$

$$\mathrm{GUE}_n = \mathrm{even}(\mathrm{GOE}_n \cup \mathrm{GOE}_{n+1}). \qquad\qquad (6.13b)$$

The meaning is as follows: First, the statistics of the ordered eigenvalues of the n-dimensional GSE is the same as that of the even numbered ordered eigenvalues of the $2n + 1$-dimensional GOE. Second, the statistics of the ordered eigenvalues of the n-dimensional GUE is the same as that of the even numbered ordered levels obtained from joining the eigenvalues of a n-dimensional GOE with the eigenvalues of a statistically independent $n + 1$-dimensional GOE.

Now, (6.13a) readily implies, in the soft edge scaling limit (2.4), that the cumulative distribution function of the k-th largest eigenvalue in GSE agrees with the cumulative distribution function of the $2k$-th largest of GOE,

$$F_4(k;s) = F_1(2k;s) \qquad (k = 1, 2, 3, \ldots), \qquad\qquad (6.14)$$

the so-called *interlacing property*. Therefore, in view of (6.1) and (6.9) we get

$$\tilde{E}_1(2k;s) + \tilde{E}_1(2k+1;s) = \tfrac{1}{2}(\tilde{E}_+(k;s) + \tilde{E}_-(k;s)). \qquad (6.15)$$

Further, the combinatorics of (6.13b) implies, in the soft edge scaling limit (2.4): exactly k levels of GUE are larger than s if and only if exactly $2k$ or $2k + 1$ levels of the union of GOE with itself are larger than s. Here, j levels are from the first copy of GOE and $2k - j$, or $2k + 1 - j$, are from the second copy. Since all of these events are mutually exclusive, we get

$$\tilde{E}_2(k;s) = \sum_{j=0}^{2k} \tilde{E}_1(j;s)\tilde{E}_1(2k-j;s) + \sum_{j=0}^{2k+1} \tilde{E}_1(j;s)\tilde{E}_1(2k+1-j;s). \qquad (6.16)$$

Finally, the following theorem gives the desired (recursive) formulae for the functions $\tilde{E}_1(k;s)$ in terms of $\tilde{E}_\pm(k;s)$. Note that these recursion formulae, though being quite different from (5.8), share the separation into even and odd numbered cases.

---

[14]That is why we have chosen, in defining the Gaussian ensembles, the same variances of the Gaussian weights as Forrester and Rains (2001).

Theorem 6.2. *The system (6.7), (6.8a), (6.15), and (6.16) of functional equations has the unique, recursively defined solution*

$$\tilde{E}_1(2k;s) = \tilde{E}_+(k;s) - \sum_{j=0}^{k-1} \frac{\binom{2j}{j}}{2^{2j+1}(j+1)} \tilde{E}_1(2k - 2j - 1;s), \tag{6.17a}$$

$$\tilde{E}_1(2k + 1;s) = \frac{\tilde{E}_+(k;s) + \tilde{E}_-(k;s)}{2} - \tilde{E}_1(2k;s). \tag{6.17b}$$

Proof. We introduce the generating functions

$$f_{\text{even}}(x) = \sum_{k=0}^{\infty} \tilde{E}_1(2k;s)x^{2k} \tag{6.18a}$$

$$f_{\text{odd}}(x) = \sum_{k=0}^{\infty} \tilde{E}_1(2k + 1;s)x^{2k} \tag{6.18b}$$

$$g_{\pm}(x) = \sum_{k=0}^{\infty} \tilde{E}_{\pm}(k;s)x^{2k}. \tag{6.18c}$$

Ferrari and Spohn's (2005) representation (6.8a) translates into the constant term equality (which breaks the symmetry of the other functional equations)

$$f_{\text{even}}(0) = g_+(0). \tag{6.19}$$

Equating (6.7) and (6.16) translates into

$$f_{\text{even}}(x)^2 + 2f_{\text{even}}(x)f_{\text{odd}}(x) + x^2 f_{\text{odd}}(x)^2 = g_+(x) \cdot g_-(x). \tag{6.20}$$

Finally, (6.15) translates into

$$f_{\text{even}}(x) + f_{\text{odd}}(x) = \tfrac{1}{2}(g_+(x) + g_-(x)). \tag{6.21}$$

Elimination of g_- from the last two equations results in the quadratic equation

$$(f_{\text{even}}(x) - g_+(x))^2 + 2(f_{\text{even}}(x) - g_+(x))f_{\text{odd}}(x) + x^2 f_{\text{odd}}(x)^2 = 0. \tag{6.22}$$

Solving for $f_{\text{even}}(x) - g_+(x)$ gives the two possible solutions

$$f_{\text{even}}(x) - g_+(x) = -\left(1 \pm \sqrt{1 - x^2}\right) f_{\text{odd}}(x). \tag{6.23}$$

Because of $f_{\text{odd}}(0) = \tilde{E}_1(1;s) > 0$ we have to choose the negative sign of the square root to satisfy (6.19). To summarize, we have obtained the mutual relations

$$f_{\text{even}}(x) = g_+(x) - \left(1 - \sqrt{1 - x^2}\right) f_{\text{odd}}(x), \tag{6.24a}$$

$$f_{\text{odd}}(x) = \tfrac{1}{2}(g_+(x) + g_-(x)) - f_{\text{even}}(x), \tag{6.24b}$$

which then, by the Maclaurin expansion

$$1 - \sqrt{1 - x^2} = \sum_{j=0}^{\infty} \frac{\binom{2j}{j}}{2^{2j+1}(j+1)} x^{2j+2}, \tag{6.25}$$

translate back into the asserted recursion formulae of the theorem. $\qquad\square$

a. density $\partial_s F_1(k;s)$ of k-th largest level in GOE   b. absolute error of Dieng's (2005) evaluation
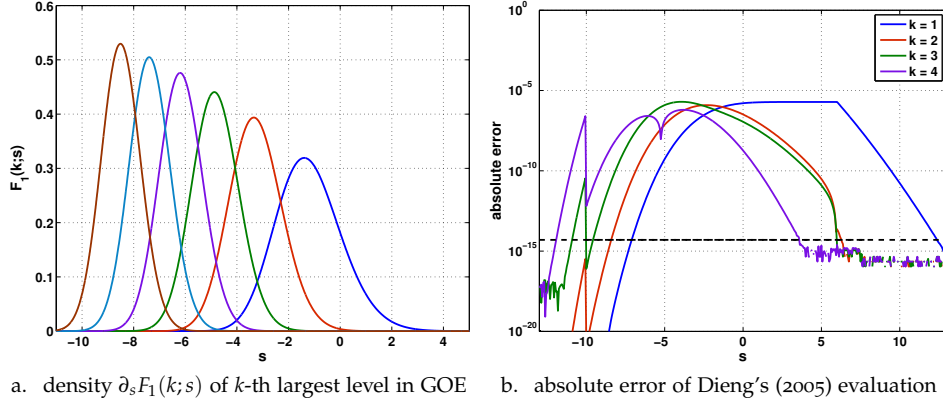
FIGURE 6. Left: plots of the probability densities of the k-th largest level in the soft edge scaling limit of GOE ($k = 1, \ldots, 6$; larger k go to the left) based on the recursion formulae (6.17). The underlying calculations were all done in hardware arithmetic and are accurate to an absolute error of about $5 \cdot 10^{-15}$ (dashed line). Right: the absolute error (taking the values of the calculations on the left as reference) of the Painlevé II based calculations by Dieng (2005).

Remark 6.3. The system (6.24) can readily be solved for $f_{\mathrm{even}}(x)$ and $f_{\mathrm{odd}}(x)$ to yield

$$\sum_{k=0}^{\infty} \tilde{E}_1(k;s)x^k = f_{\mathrm{even}}(x) + x f_{\mathrm{odd}}(x)$$

$$= \frac{1}{2}\left(g_+(x)\left(1 + \sqrt{\frac{1-x}{1+x}}\right) + g_-(x)\left(1 - \sqrt{\frac{1-x}{1+x}}\right)\right). \quad (6.26)$$

In view of (2.19) this implies the determinantal equation (cf., after squaring, Forrester 2006, Eq. (1.22))

$$D_1(z;(s,\infty))^{1/2} = \frac{1}{2}\left(\det\left(I - \sqrt{z(2-z)}\, V_{\mathrm{Ai}}\!\restriction_{L^2(s,\infty)} \right)\left(1 + \sqrt{\frac{z}{2-z}}\right)\right.$$

$$\left. + \det\left(I + \sqrt{z(2-z)}\, V_{\mathrm{Ai}}\!\restriction_{L^2(s,\infty)} \right)\left(1 - \sqrt{\frac{z}{2-z}}\right)\right) \quad (6.27)$$

for all $s \in \mathbb{R}$ and z in the complex domain of analyticity that contains $z = 1$. This formula thus paves, following the arguments of the proof of Theorem 6.1, an elementary road to the Painlevé representation (Dieng 2005, Eq. (1.2.1)) of $D_1(z;(s,\infty))$ (see also Forrester 2006, Eq. (1.17)).

Based on the recursion formulae (6.17) and the numerical methods of Section 4 we calculated the distribution functions $F_1(k;s)$ of the k-th largest level in the soft edge scaling limit of GOE—note that because of (6.14) there is no need for a separate calculation of the corresponding distributions $F_4(k;s)$ for GSE. The corresponding densities are shown, for $k = 1, \ldots, 6$, in Figure 6.a. These

calculations are accurate to the imposed absolute tolerance of $5 \cdot 10^{-15}$. Taking our numerical solutions as reference, Figure 6.b shows the absolute error of the Painlevé II based numerical evaluations by Dieng (2005), which are available for $k = 1, \ldots, 4$. Perfectly visible are the points $a_+ = -10$ and $b_- = 6$ where Dieng chose to switch from an asymptotic formula to the BVP solution of Painlevé II, see Section 3.2.1.

7. The k-th Smallest Level at the Hard Edge: LOE and LSE

In this section we derive determinantal formulae for the cumulative distribution functions $F_{\beta,\alpha}(k;s)$ of the k-th smallest level in the hard edge scaling limit of LOE, LUE, and LSE with parameter α. It turns out that these formulae have the same *algebraic* structure as those developed for the k-th largest level in the soft edge scaling limit. Therefore, though more concise, we proceed step-by-step in parallel to the arguments of the preceding section.

By the underlying combinatorial structure we have

$$F_{\beta,\alpha}(k;s) = 1 - \sum_{j=0}^{k-1} E_{\beta,\alpha}(j;s), \tag{7.1}$$

where we briefly write

$$E_{\beta,\alpha}(k;s) = E_\beta^{(\mathrm{hard})}(k;(0,s),\alpha). \tag{7.2}$$

The integral representation

$$K_\alpha(x,y) = \frac{1}{4} \int_0^1 J_\alpha\left(\sqrt{\xi}x\right) J_\alpha\left(\sqrt{\xi}y\right) d\xi \tag{7.3}$$

of the Bessel kernel implies, by introducing the kernels

$$T_{s,\alpha}(x,y) = \frac{\sqrt{s}}{2} J_\alpha\left(\sqrt{sxy}\right), \qquad V_\alpha(x,y) = \frac{1}{2} J_\alpha\left(\sqrt{xy}\right), \tag{7.4}$$

the factorization

$$\det\left(I - zK_\alpha\restriction_{L^2(0,s)}\right) = \det\left(I - z\left(T_{s,\alpha}\restriction_{L^2(0,1)}\right)^2\right)$$

$$= \det\left(I - \sqrt{z}\,T_{s,\alpha}\restriction_{L^2(0,1)}\right) \cdot \det\left(I + \sqrt{z}\,T_{s,\alpha}\restriction_{L^2(0,1)}\right)$$

$$= \det\left(I - \sqrt{z}\,V_\alpha\restriction_{L^2(0,\sqrt{s})}\right) \cdot \det\left(I + \sqrt{z}\,V_\alpha\restriction_{L^2(0,\sqrt{s})}\right) \tag{7.5}$$

that is valid for the complex cut plane $z \in \mathbb{C} \setminus (-\infty, 0]$. Now, upon introducing the functions

$$E_{\pm,\alpha}(k;s) = \frac{(-1)^k}{k!} \frac{d^k}{dz^k} \det\left(I \mp \sqrt{z}\,V_\alpha\restriction_{L^2(0,\sqrt{s})}\right)\bigg|_{z=1} \tag{7.6}$$

we obtain from (2.39)

$$E_{2,\alpha}(k;s) = \sum_{j=0}^k E_{+,\alpha}(j;s)E_{-,\alpha}(k-j;s). \tag{7.7}$$

Desrosiers and Forrester (2006, Prop. 1) proved that

$$E_{1,\frac{\alpha-1}{2}}(0;s) = E_{+,\alpha}(0;s) \tag{7.8a}$$

$$E_{4,\alpha+1}(0;s) = \tfrac{1}{2}(E_{+,\alpha}(0;s) + E_{-,\alpha}(0;s)). \tag{7.8b}$$

The last generalizes to

$$E_{4,\alpha+1}(k;s) = \tfrac{1}{2}(E_{+,\alpha}(k;s) + E_{-,\alpha}(k;s)) \qquad (k = 0, 1, 2, \ldots), \tag{7.9}$$

or, equivalently, to the generating function

$$\sum_{k=0}^{\infty} E_{4,\alpha+1}(k;s)(1-z)^k$$
$$= \frac{1}{2}\left(\det\left(I - \sqrt{z}\, V_\alpha\!\upharpoonright_{L^2(0,\sqrt{s})}\right) + \det\left(I + \sqrt{z}\, V_\alpha\!\upharpoonright_{L^2(0,\sqrt{s})}\right)\right) \tag{7.10}$$

that holds for all $s \in (0,\infty)$ and z in the complex domain of analyticity that contains $z = 1$. A proof of (7.10), using Painlevé representations, was given by Forrester (2006, Eq. (1.38)).

It remains to discuss the LOE. To this end we use the interrelationships between LOE, LUE, and LSE found by Forrester and Rains (2001, Thms. 4.3/5.1),[15] which can symbolically be written in the form

$$\mathrm{LSE}_{n,\alpha+1} = \mathrm{even}\left(\mathrm{LOE}_{2n+1,\frac{\alpha-1}{2}}\right), \tag{7.11a}$$

$$\mathrm{LUE}_{n,\alpha} = \mathrm{even}\left(\mathrm{LOE}_{n,\frac{\alpha-1}{2}} \cup \mathrm{LOE}_{n+1,\frac{\alpha-1}{2}}\right). \tag{7.11b}$$

Here, we write $\mathrm{LOE}_{n,\alpha}$ for the n-dimensional LOE with parameter α, etc. Otherwise, these symbolic equations have the same meaning as (6.13a) and (6.13b). For the same purely combinatorial reasons as in the preceding section we hence get

$$F_{4,\alpha+1}(k;s) = F_{1,\frac{\alpha-1}{2}}(2k;s) \qquad (k = 1, 2, 3, \ldots), \tag{7.12}$$

or, equivalently by (7.1) and (7.9),

$$E_{1,\frac{\alpha-1}{2}}(2k;s) + E_{1,\frac{\alpha-1}{2}}(2k+1;s) = \tfrac{1}{2}(E_{+,\alpha}(k;s) + E_{-,\alpha}(k;s)), \tag{7.13}$$

as well as (see also Forrester 2006, Cor. 4)

$$E_{2,\alpha}(k;s)$$
$$= \sum_{j=0}^{2k} E_{1,\frac{\alpha-1}{2}}(j;s)E_{1,\frac{\alpha-1}{2}}(2k-j;s) + \sum_{j=0}^{2k+1} E_{1,\frac{\alpha-1}{2}}(j;s)E_{1,\frac{\alpha-1}{2}}(2k+1-j;s). \tag{7.14}$$

Since Theorem 6.2 was in fact just addressing the solution of a specific system of functional equations, we obtain the same result here because the system (7.7), (7.8a), (7.13), and (7.14) possesses exactly the algebraic structure considered there.

---

[15]Again, that is why we have chosen the weight functions scaled as in Forrester and Rains (2001).

That is, we get the solution

$$E_{1,\frac{\alpha-1}{2}}(2k;s) = E_{+,\alpha}(k;s) - \sum_{j=0}^{k-1} \frac{\binom{2j}{j}}{2^{2j+1}(j+1)} E_{1,\frac{\alpha-1}{2}}(2k-2j-1;s), \quad (7.15a)$$

$$E_{1,\frac{\alpha-1}{2}}(2k+1;s) = \frac{E_{+,\alpha}(k;s) + E_{-,\alpha}(k;s)}{2} - E_{1,\frac{\alpha-1}{2}}(2k;s). \quad (7.15b)$$

and, completely parallel to (6.27), the corresponding generating function

$$\sum_{k=0}^{\infty} E_{1,\frac{\alpha-1}{2}}(k;s)(1-z)^k = \frac{1}{2}\left(\det\left(I - \sqrt{z(2-z)}\, V_\alpha\!\restriction_{L^2(0,\sqrt{s})} \right)\left(1 + \sqrt{\frac{z}{2-z}} \right) \right.$$

$$\left. + \det\left(I + \sqrt{z(2-z)}\, V_\alpha\!\restriction_{L^2(0,\sqrt{s})} \right)\left(1 - \sqrt{\frac{z}{2-z}} \right) \right) \quad (7.16)$$

for all $s \in (0,\infty)$ and z in the complex domain of analyticity that contains $z = 1$.

Remark 7.1. Given the large order asymptotics (Olver 1974, Eq. (9.5.01))

$$J_\alpha(\alpha + \zeta\alpha^{1/3}) = 2^{1/3}\alpha^{-1/3}\mathrm{Ai}(-2^{1/3}\zeta) + O(\alpha^{-1}) \qquad (\alpha \to \infty), \quad (7.17)$$

which holds uniformly for bounded ζ, we get, by changing variables subject to

$$x = \sqrt{\alpha^2 - 2\alpha(\alpha/2)^{1/3}\xi}, \qquad y = \sqrt{\alpha^2 - 2\alpha(\alpha/2)^{1/3}\eta}, \quad (7.18)$$

the kernel approximation

$$V_\alpha(x,y)\frac{dy}{d\eta} = -V_{\mathrm{Ai}}(\xi,\eta) + O(\alpha^{-2/3}) \qquad (\alpha \to \infty), \quad (7.19)$$

uniformly for bounded ξ, η. Since $y = 0$ is mapped to $\eta = (\alpha/2)^{2/3} \to \infty$ $(\alpha \to \infty)$ we therefore obtain, observing the fast decay of the Bessel and Airy functions, the operator approximation (in trace class norm)

$$V_\alpha\!\restriction_{L^2\left(0,\sqrt{\alpha^2-2\alpha(\alpha/2)^{1/3}s}\right)} = V_{\mathrm{Ai}}\!\restriction_{L^2(s,\infty)} + O(\alpha^{-2/3}) \qquad (\alpha \to \infty). \quad (7.20)$$

This approximation implies the limit of the associated Fredholm determinants,

$$\lim_{\alpha\to\infty} \det\left(I - zV_\alpha\!\restriction_{L^2\left(0,\sqrt{\alpha^2-2\alpha(\alpha/2)^{1/3}s}\right)} \right) = \det\left(I - zV_{\mathrm{Ai}}\!\restriction_{L^2(s,\infty)} \right), \quad (7.21)$$

or, equivalently,

$$\lim_{\alpha\to\infty} E_{\pm,\alpha}(k;\alpha^2 - 2\alpha(\alpha/2)^{1/3}s) = \tilde{E}_\pm(k;s) \qquad (k = 0,1,2,\ldots). \quad (7.22)$$

Plugging this limit into (7.7), (7.9), and (7.15) yields, by (6.7), (6.9), and (6.17), the hard-to-soft transition (see also Borodin and Forrester 2003, §4)

$$\lim_{\alpha\to\infty} E_{\beta,\alpha(\beta)}(k;\alpha^2 - 2\alpha(\alpha/2)^{1/3}s) = \tilde{E}_\beta(k;s) \quad (7.23)$$

with

$$\alpha(\beta) = \begin{cases} (\alpha-1)/2, & \beta = 1, \\ \alpha, & \beta = 2, \\ \alpha+1, & \beta = 4. \end{cases} \quad (7.24)$$

This transition is a further convenient mean to validate our numerical methods.

8. Matrix Kernels and Examples of Joint Probability Distributions

8.1. **Matrix Kernels.** Bornemann (2010a, §8.1) showed that the quadrature based approach to the numerical approximation of Fredholm determinants that we described in Section 4.1, can fairly easily be extended to matrix kernel determinants of the form

$$d(z) = \det \left(I - z \begin{pmatrix} K_{11} & \cdots & K_{1N} \\ \vdots & & \vdots \\ K_{N1} & \cdots & K_{NN} \end{pmatrix} \restriction_{L^2(J_1) \oplus \cdots \oplus L^2(J_N)} \right), \tag{8.1}$$

where $J_1, \ldots, J_N$ are open intervals and the smooth matrix kernel generates a trace class operator on $L^2(J_1) \oplus \cdots \oplus L^2(J_N)$. By taking an m-point quadrature rule of order m with nodes $x_{ij} \in J_i$ and *positive* weights w_{ij}, written in the form

$$\sum_{j=1}^{m} w_{ij} f(x_{ij}) \approx \int_{J_i} f(x) \, dx \qquad (i = 1, \ldots, N), \tag{8.2}$$

we approximate $d(z)$ by the $N \cdot m$-dimensional determinant

$$d_m(z) = \det \left(I - z \begin{pmatrix} A_{11} & \cdots & A_{1N} \\ \vdots & & \vdots \\ A_{N1} & \cdots & A_{NN} \end{pmatrix} \right) \tag{8.3a}$$

with block entries A_{ij} that are the $m \times m$ matrices given by

$$(A_{ij})_{p,q} = w_{ip}^{1/2} K_{ij}(x_{ip}, x_{jq}) w_{jq}^{1/2} \qquad (p = 1, \ldots, m; q = 1, \ldots, m). \tag{8.3b}$$

If the kernel functions $K_{ij}(x, y)$ are analytic in a complex neighborhood of $J_i \times J_j$, one can prove exponential convergence (Bornemann 2010a, Thm. 8.1): there is a constant $\rho > 1$ such that

$$d_m(z) - d(z) = O(\rho^{-m}) \qquad (m \to \infty), \tag{8.4}$$

locally uniform in $z \in \mathbb{C}$. The results of Section 4.2–4.5 apply then verbatim. This approach was used to evaluate the matrix kernel determinant (2.16) for the numerical checks of the fundamental equation (6.10) in Section 6.
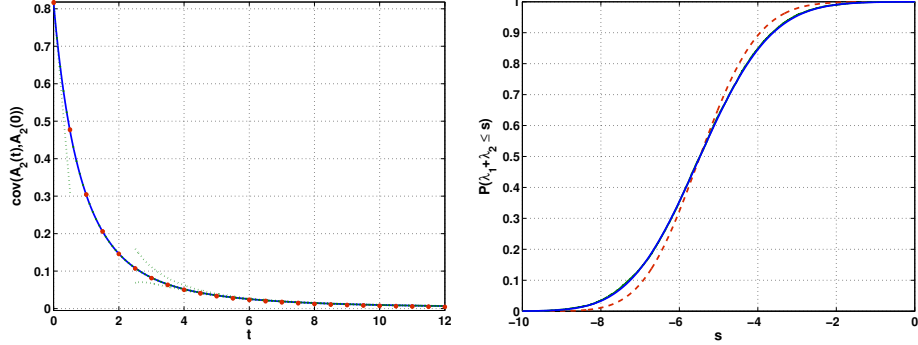
8.1.1. *An example: the joint probability distribution of GUE matrix diffusion.* Prähofer and Spohn (2002) proved that the joint probability of the maximum eigenvalue of GUE matrix diffusion at two different times is given, in the soft edge scaling limit, by the operator determinant

$$\mathbb{P}(\mathcal{A}_2(t) \leqslant s_1, \mathcal{A}_2(0) \leqslant s_2) = \det \left(I - \begin{pmatrix} K_0 & K_t \\ K_{-t} & K_0 \end{pmatrix} \restriction_{L^2(s_1,\infty) \oplus L^2(s_2,\infty)} \right) \tag{8.5a}$$

with kernel

$$K_t(x, y) = \begin{cases} \displaystyle\int_0^\infty e^{-\xi t} \mathrm{Ai}(x + \xi) \mathrm{Ai}(y + \xi) \, d\xi & (t \geqslant 0), \\[2ex] \displaystyle -\int_{-\infty}^0 e^{-\xi t} \mathrm{Ai}(x + \xi) \mathrm{Ai}(y + \xi) \, d\xi & (t < 0). \end{cases} \tag{8.5b}$$

(Note that $K_0 = K_{\mathrm{Ai}}$, see (6.3).) This expression is directly amenable to our numerical methods; Figure 7.a shows the covariance function that was calculated this

a. $\mathrm{cov}(\mathcal{A}_2(t), \mathcal{A}_2(0))$ for GUE matrix diffusion   b.   CDF of the sum of largest two levels in GUE

FIGURE 7. Left: plot (blue line) of the covariance $\mathrm{cov}(\mathcal{A}_2(t), \mathcal{A}_2(0))$ of the maximum eigenvalue of GUE matrix diffusion at two different times (soft edge scaling limit), calculated from the joint probability distribution (8.5) to 10 digits accuracy (absolute tolerance $5 \cdot 10^{-11}$). The red dots show the data obtained from a Monte Carlo simulation with matrix dimensions $m = 128$ and $m = 256$ (there is no difference visible between the two dimensions on the level of plotting accuracy). The dashed, green lines show the asymptotic expansions (8.6) and (8.7). Right: plot (blue line) of the CDF (8.24) of the sum of the largest two levels of GUE (soft edge scaling limit), calculated from the joint probability distribution (8.22) to 10 digits accuracy (absolute tolerance $5 \cdot 10^{-11}$). To compare with, we also show (red, dashed line) the convolution (8.25) of the corresponding individual CDFs from Figure 4.b; because of statistical dependence, there is a clearly visible difference.

way. The results were cross-checked with a Monte Carlo simulation (red dots), and with the help of the following asymptotic expansions (dashed lines): for small t with the expansion (Prähofer and Spohn 2002, Hägg 2008)

$$\mathrm{cov}(\mathcal{A}_2(t), \mathcal{A}_2(0)) = \mathrm{var}(F_2) - t + O(t^2) \qquad (t \to 0), \qquad (8.6)$$

where F_2 denotes the Tracy–Widom distribution for GUE (the numerical value of $\mathrm{var}(F_2)$ can be found in Table 4); for large t with the expansion (Widom 2004, Adler and van Moerbeke 2005)

$$\mathrm{cov}(\mathcal{A}_2(t), \mathcal{A}_2(0)) = t^{-2} + ct^{-4} + O(t^{-6}) \qquad (t \to \infty), \qquad (8.7)$$

where the constant $c = -3.542\cdots$ can explicitly be expressed in terms of the Hastings–McLeod solution (1.8) of Painlevé II.

Similar calculations related to GOE matrix diffusion, and their impact on "experimentally disproving" a conjectured determinantal formula, are discussed in a recent paper by Bornemann, Ferrari and Prähofer (2008).

Remark. In a masterful analytic study, Adler and van Moerbeke (2005) proved that the function $G(t, x, y) = \log \mathbb{P}(\mathcal{A}_2(t) \leqslant x, \mathcal{A}_2(0) \leqslant y)$ satisfies the following

nonlinear 3rd order partial differential equation (together with certain asymptotic boundary conditions):

$$t\frac{\partial}{\partial t}\left(\frac{\partial^2}{\partial x^2}-\frac{\partial^2}{\partial y^2}\right)G = \frac{\partial^3 G}{\partial x^2\partial y}\left(2\frac{\partial^2 G}{\partial y^2}+\frac{\partial^2 G}{\partial x\partial y}-\frac{\partial^2 G}{\partial x^2}+x-y-t^2\right)$$

$$-\frac{\partial^3 G}{\partial y^2\partial x}\left(2\frac{\partial^2 G}{\partial x^2}+\frac{\partial^2 G}{\partial x\partial y}-\frac{\partial^2 G}{\partial y^2}-x+y-t^2\right)$$

$$+\left(\frac{\partial^3 G}{\partial x^3}\frac{\partial}{\partial y}-\frac{\partial^3 G}{\partial y^3}\frac{\partial}{\partial x}\right)\left(\frac{\partial}{\partial x}+\frac{\partial}{\partial y}\right)G. \quad (8.8)$$

The reader should contemplate a numerical calculation of the covariance function based on this PDE, rather than directly treating the Fredholm determinant (8.5) as suggested in this paper.

8.2. **Operators Acting on Unions of Intervals.** Determinants of integral operators K acting on the space $L^2(J_1\cup\cdots\cup J_N)$ of functions defined on a union of mutually *disjoint* open intervals can be dealt with by transforming them to a matrix kernel determinant (Gohberg, Goldberg and Krupnik 2000, Thm. VI.6.1):

$$\det\left(I - zK\restriction_{L^2(J_1\cup\cdots\cup J_N)}\right)$$

$$= \det\left(I - z\begin{pmatrix} K_{11} & \cdots & K_{1N} \\ \vdots & & \vdots \\ K_{N1} & \cdots & K_{NN} \end{pmatrix}\restriction_{L^2(J_1)\oplus\cdots\oplus L^2(J_N)}\right), \quad (8.9)$$

where $K_{ij} : L^2(J_j) \to L^2(J_i)$ denotes the integral operator induced by the given kernel function $K(x,y)$, that is,

$$K_{ij}u(x) = \int_{J_j} K(x,y)u(y)\,dy \qquad (x\in J_i). \quad (8.10)$$

More general, along the same lines, with χ_J denoting the characteristic function of an interval J and $z_j\in\mathbb{C}$, we have

$$\det\left(I - \left(K\sum_{j=1}^{N} z_j\chi_{J_j}\right)\restriction_{L^2(\mathbb{R})}\right)$$

$$= \det\left(I - \begin{pmatrix} z_1 K_{11} & \cdots & z_N K_{1N} \\ \vdots & & \vdots \\ z_1 K_{N1} & \cdots & z_N K_{NN} \end{pmatrix}\restriction_{L^2(J_1)\oplus\cdots\oplus L^2(J_N)}\right), \quad (8.11)$$

where the $K_{ij} : L^2(J_j) \to L^2(J_i)$ denote, once more, the integral operators defined in (8.10). To indicate the fact that the operators K_{ij} share one and the same kernel function $K(x,y)$ we also write, by "abus d'langage",

$$\det\left(I - z\begin{pmatrix} K & \cdots & K \\ \vdots & & \vdots \\ K & \cdots & K \end{pmatrix}\restriction_{L^2(J_1)\oplus\cdots\oplus L^2(J_N)}\right) \quad (8.12)$$

for (8.9) and

$$\det \left(I - \begin{pmatrix} z_1 K & \cdots & z_N K \\ \vdots & & \vdots \\ z_1 K & \cdots & z_N K \end{pmatrix} \restriction_{L^2(J_1) \oplus \cdots \oplus L^2(J_N)} \right) \tag{8.13}$$

for (8.11). Clearly, in both of the cases (8.9) and (8.11), we then apply the method of Section 8.1 for the numerical evaluation of the equivalent matrix kernel determinant.

8.3. **Generalized Spacing Functions.** The determinantal formulae (2.11), (2.14), (2.15), (2.16), (2.36), and (2.39) have all the common form

$$E(k; J) = \mathbb{P}(\text{exactly } k \text{ levels lie in } J) = \frac{(-1)^k}{k!} \frac{d^k}{dz^k} \det \left(I - z\, K \restriction_{L^2(J)} \right) \bigg|_{z=1}, \tag{8.14}$$

which is based on an underlying combinatorial structure that can be extended to describe, for a multi-index $\alpha \in \mathbb{N}_0^N$ and mutually *disjoint* open intervals J_j $(j = 1, \ldots, N)$, the generalized spacing function

$$E(\alpha; J_1, \ldots, J_N) = \mathbb{P}(\text{exactly } \alpha_j \text{ levels lie in } J_j, j = 1, \ldots, N) \tag{8.15a}$$

by the determinantal formula (see Tracy and Widom (1993a), Thm. 6, or (1998), Eq. (4.1))

$$\begin{aligned} E(\alpha; J_1, \ldots, J_N) \\ = \frac{(-1)^{|\alpha|}}{\alpha!} \frac{\partial^\alpha}{\partial z^\alpha} \det \left(I - \left(K \sum_{j=1}^N z_j \chi_{J_j} \right) \restriction_{L^2(\mathbb{R})} \right) \bigg|_{z_1 = \cdots = z_N = 1}. \end{aligned} \tag{8.15b}$$

By the results of Section 8.2 and 4.3, such an expression is, in principle at least, amenable to the numerical methods of this paper. However, differentiation with respect to l different variables z_j means to evaluate an l-dimensional Cauchy integral of a function that is calculated from approximating a Fredholm determinant. This can quickly become very expensive, indeed.

8.3.1. *Efficient numerical evaluation of the finite-dimensional determinants.* Let us briefly discuss the way one would adapt the methods of Section 4.2 to the current situation. We will confine ourselves to the important case of a multi-index α which has the form $\alpha = (k, 0, \ldots, 0)$. If we are to compute the derivatives by a Cauchy integral, we have to evaluate a determinant of the form[16]

$$d(z) = \det(I - (zA \mid B)) \qquad A \in \mathbb{R}^{m,p}, B \in \mathbb{R}^{m,m-p} \tag{8.16}$$

for several different arguments $z \in \mathbb{C}$. By putting

$$T = I - (0 \mid B), \qquad \tilde{A} = T^{-1}(A \mid 0), \tag{8.17}$$

we have $I - (zA \mid B) = T(I - z\tilde{A})$ and hence the factorization

$$d(z) = \det(T) \cdot \det(I - z\tilde{A}) \tag{8.18}$$

to which the results of Section 4.2 apply verbatim.

---

[16]Which is understood to be an approximation of the determinant in (8.15), expressed as the matrix kernel determinant (8.11).

8.3.2. *An example: the joint distribution of the largest two eigenvalues in GUE.* Let us denote by λ_1 the largest and by λ_2 the second largest level of GUE in the soft edge scaling limit (2.4). We want to evaluate their joint probability distribution function

$$F(x,y) = \mathbb{P}(\lambda_1 \leqslant x, \lambda_2 \leqslant y). \tag{8.19}$$

Since $\lambda_1 \leqslant x \leqslant y$ certainly implies $\lambda_2 \leqslant y$, we have

$$F(x,y) = \mathbb{P}(\lambda_1 \leqslant x) = F_2(x) \qquad (x \leqslant y). \tag{8.20}$$

On the other hand, if $x > y$, the open intervals (y,x) and (x,∞) are disjoint and we obtain for simple combinatorial reasons

$$F(x,y) = E_2^{(\text{soft})}(0,0;(y,x),(x,\infty)) + E_2^{(\text{soft})}(1,0;(y,x),(x,\infty))$$

$$= E_2^{(\text{soft})}(0;(y,\infty)) + E_2^{(\text{soft})}(1,0;(y,x),(x,\infty))$$

$$= F_2(y) + E_2^{(\text{soft})}(1,0;(y,x),(x,\infty)) \qquad (x > y). \tag{8.21}$$

By (8.15) and (8.11) we finally get

$$F(x,y)$$

$$= \begin{cases} F_2(x) & (x \leqslant y), \\ F_2(y) - \dfrac{\partial}{\partial z} \det\left(I - \begin{pmatrix} z\,K_{\text{Ai}} & K_{\text{Ai}} \\ z\,K_{\text{Ai}} & K_{\text{Ai}} \end{pmatrix}\Big\lceil_{L^2(y,x)\oplus L^2(x,\infty)}\right)\Bigg|_{z=1} & (x > y). \end{cases} \tag{8.22}$$

We have used this formula to calculate the correlation of the largest two levels as

$$\rho(\lambda_1,\lambda_2) = 0.50564\,723159\ldots; \tag{8.23}$$

where all the 11 digits shown are estimated to be correct and the run time was about 16 hours using hardware arithmetic.[17] So, as certainly was to be expected, the largest two levels are statistically very much *dependent*. Figure 7.b plots the CDF of the sum of the largest two levels,

$$\mathbb{P}(\lambda_1 + \lambda_2 \leqslant s) = \int_{-\infty}^{\infty} \partial_1 F(x,s-x)\,dx, \tag{8.24}$$

and compares the result with the convolution of the individual CDFs of these levels, that is with the s-dependent function

$$\int_{-\infty}^{\infty} F_2'(1;x)F_2(2;s-x)\,dx. \tag{8.25}$$

The clearly visible difference between those two functions is a further corollary of the statistical dependence of the largest two level.

Yet another calculation of joint probabilities in the spectrum of GUE (namely, related to the statistical *independence* of the extreme eigenvalues) can be found in Bornemann (2010b).

---

[17]So, this example stretches our numerical methods pretty much to the edge of what is possible. Note, however, that these numerical results are completely out of the reach of a representation by partial differential equations.

TABLE 5. Toolbox commands for kernel functions $K(x, y)$. If the value of $K(x, y)$ is defined as an integral, there is an additional argument m to the command that assigns the number of quadrature points to be used.

kernel	formula	command	vectorization mode
$K_{\sin}(x, y)$	(1.2)	`sinc(pi*(x-y))`	`'grid'`
$V_{Ai}(x, y)$	(6.4)	`airy((x+y)/2)/2`	`'grid'`
$V_{\alpha}(x, y)$	(7.4)	`besselj(alpha,sqrt(x.*y))/2`	`'grid`
$K_n(x, y)$	(2.12)	`HermiteKernel(n,x,y)`	`'outer'`
$K_{Ai}(x, y)$	(1.6)	`AiryKernel(x,y)`	`'outer'`
$K_{n,\alpha}(x, y)$	(2.37)	`LaguerreKernel(n,alpha,x,y)`	`'outer'`
$K_{\alpha}(x, y)$	(2.39c)	`BesselKernel(alpha,x,y)`	`'outer'`
$S(x, y)$	(2.17a)	`F4MatrixKernel(x,y,m,'SN')`	`'outer'`
$S^*(x, y)$	(2.17a)	`F4MatrixKernel(x,y,m,'ST')`	`'outer'`
$SD(x, y)$	(2.17b)	`F4MatrixKernel(x,y,m,'SD')`	`'outer'`
$IS(x, y)$	(2.17c)	`F4MatrixKernel(x,y,m,'IS')`	`'outer'`
$K_t(x, y)$	(8.5b)	`Airy2ProcessKernel(t,x,y,m)`	`'outer'`

9. SOFTWARE

We have coded the numerical methods of this paper in a Matlab toolbox. (For the time being, it can be obtained from the author upon request by e-mail. At a later stage it will be made freely available at the web.) In this section we explain the design and use of the toolbox.

9.1. **Low Level Commands.**

9.1.1. *Quadrature rule.* The command

```
>> [w,x] = ClenshawCurtis(a,b,m)
```

calculates the *m*-point Clenshaw–Curtis quadrature rules (suitably transformed if $a = -\infty$ or $b = \infty$). The result is a row vector w of weights and a column vector x of nodes. This way, the application (4.1) of the quadrature rule to a (vectorizing) function f goes simply by the following command:

```
>> w*f(x)
```

Once called for a specific number *m*, the (untransformed) weights and nodes are cached for later use. As an alternative the toolbox also offers Gauss–Jacobi quadrature, see Section A.1 for its use in the context of algebraic kernel singularities.

9.1.2. *Kernels and vectorization modes.* The numerical approximation of Fredholm determinants, by (4.3) or (8.3), requires the ability to build, for given *m*-dimensional

column vectors x and y, the $m \times m$ matrix

$$A = (K(x_i, y_j))_{i,j=1}^m.$$

For reasons of efficiency we make a meticulous use of Matlab's vectorization capabilities. Depending on the specific structure of the coding of the kernel function, we distinguish between two vectorization modes:

(1) 'grid': The matrix A is built from the vectors x, y and the kernel function K by the commands

```
>> [X,Y] = ndgrid(x,y);
>> A = K(X,Y);
```

(2) 'outer': The matrix A is built from the vectors x, y and the kernel function K by the commands

```
>> A = K(x,y);
```

Table 5 gives the commands for all the kernels used in this paper together with their vectorization modes.

9.1.3. *Approximation of Fredholm determinants.* Having built the matrix A the approximation (4.3) is finally evaluated by the following commands:

```
>> w2 = sqrt(w);
>> det(eye(size(A))-z*(w2'*w2).*A)
```

9.1.4. *Example.* Let us evaluate the values $F_1(0)$ and $F_2(0)$ of the Tracy–Widom distributions for GOE and GUE by these low level commands using $m = 64$ quadrature points. The reader should observe the different vectorization modes:

```
>> m = 64; [w,x] = ClenshawCurtis(0,inf,m); w2 = sqrt(w);
>> [xi,xj] = ndgrid(x,x);
>> K1 = @(x,y) airy((x+y)/2)/2;
>> F10 = det(eye(m)-(w2'*w2).*K1(xi,xj))

   F10 = 0.831908066202953


>> KAi = @AiryKernel;
>> F20 = det(eye(m)-(w2'*w2).*KAi(x,x))

   F20 = 0.969372828355262
```

A look into Prähofer's (2003) tables teaches that both results are correct to one unit of the last decimal place.

9.2. **Medium Level Commands.** The number of quadrature points can be hidden from the user by means of the automatic error control of Section 4.4. This means, we start thinking in terms of the limit of the approximation sequence, that is, in terms of the corresponding integral operators. This way, we evaluate the operator determinant

$$\det(I - zK\restriction_{L^2(J)})$$

for a given kernel function $K(x, y)$ by the following commands:

```
>> K.ker = @(x,y) K(x,y); k.mode = vectorizationmode;
>> Kop = op(K,J);
>> [val,err] = det1m(Kop,z);
```

(The argument z may be omitted in det1m if $z = 1$.) Here, val gives the value of the operator determinant and err is a conservative error estimate. The code tries to observe a given absolute tolerance tol that can be set by

```
>> pref('tol',tol);
```

The default is $5 \cdot 10^{-15}$, that is, tol = 5e-15. The results can be nicely printed in a way such that, within the given error, either just the correctly *rounded* decimal places are displayed (printmode = 'round'), or the correctly *truncated* places (printmode = 'trunc'):

```
>> pref('printmode',printmode);
>> PrintCorrectDigits(val,err);
```

For an integral operator *K*, the expressions

$$\frac{(-1)^k}{k!} \frac{d^k}{dz^k} \det(I - zK)\bigg|_{z=1}, \quad \frac{(-1)^k}{k!} \frac{d^k}{dz^k} \det(I - \sqrt{z}K)\bigg|_{z=1},$$

$$\frac{(-1)^k}{k!} \frac{d^k}{dz^k} \sqrt{\det(I - zK)}\bigg|_{z=1},$$

are then evaluated, with error estimate, by the following commands:

```
>> [val,err] = dzdet(K,k);
>> [val,err] = dzdet(K,k,@sqrt);
>> [val,err] = dzsqrtdet(K,k);
```

9.2.1. *Example 9.1.4 revisited.* Let us now evaluate the values $F_1(0)$ and $F_2(0)$ of the Tracy–Widom distributions for GOE and GUE by these medium level commands.

```
>> pref('printmode','trunc');
>> K1.ker = @(x,y) airy((x+y)/2)/2; K1.mode = 'grid';
>> [val,err] = det1m(op(K1,[0,inf]));
>> PrintCorrectDigits(val,err);

   0.83190806620295_

>> KAi.ker = @AiryKernel; KAi.mode = 'outer';
>> [val,err] = det1m(op(KAi,[0,inf]));
>> PrintCorrectDigits(val,err);

   0.96937282835526_
```

So, the automatic error control supposes 14 digits to be correct in both cases; a look into Prähofer's (2003) tables teaches us that this is true, indeed.

9.2.2. *Example: an instance of equation (6.10).* We now give the line of commands that we used to experimentally check the truth of the determinantal equation (6.10) before we worked out the proof. For a single instance of a real value of *s* and a complex value of *z* we obtain:

```
>> s = -1.23456789; z = -3.1415926535 + 2.7182818284i;
>>
>> K11.ker = @(x,y,m) F4MatrixKernel(x,y,m,'SN'); K11.mode = 'outer';
>> K12.ker = @(x,y,m) F4MatrixKernel(x,y,m,'SD'); K12.mode = 'outer';
>> K21.ker = @(x,y,m) F4MatrixKernel(x,y,m,'IS'); K21.mode = 'outer';
>> K22.ker = @(x,y,m) F4MatrixKernel(x,y,m,'ST'); K22.mode = 'outer';
>> K = op({K11 K12; K21 K22},{[s,inf],[s,inf]});
>> val1 = sqrt(det1m(K,z))

   val1 = 1.08629916321436 -    0.07467121693055511i


>> K1.ker = @(x,y) airy((x+y)/2)/2; K1.mode = 'grid';
>> K = op(K1,[s,inf]);
>> val2 = (det1m(K,sqrt(z)) + det1m(K,-sqrt(z)))/2

   val2 = 1.08629916321436 -    0.07467121693055508i


>> dev = abs(val1-val2)

   dev = 5.23691153334427e-016
```

This deviation is below the default tolerance $5 \cdot 10^{-15}$ which was used for the calculation.

9.3. **High Level Commands.** Using the low and medium level commands we straightforwardly coded all the functions that we have discussed in this paper so far. Table 6 lists the corresponding commands. The reader is encouraged to look into the actual code of these commands to see how closely we followed the determinantal formulae of this paper.

9.3.1. *Example 9.2.1 revisited.* Let us evaluate, for the last time in this paper, the values $F_1(0)$ and $F_2(0)$ of the Tracy–Widom distributions for GOE and GUE, now using those high level commands.

```
>> pref('printmode','trunc');
>> [val,err] = F(1,0);
>> PrintCorrectDigits(val,err);

   0.83190806620295_


>> [val,err] = F(2,0);
>> PrintCorrectDigits(val,err);

   0.96937282835526_
```

9.3.2. *Example: checking the k-level spacing functions against a constraint.* An appropriate way of checking the quality of the automatic error control goes by evaluating certain constraints such as the mass and mean given in (2.8):

TABLE 6. Toolbox commands for all the probability distributions of this paper. A call by val = E(...) etc. gives the value; with [val,err] = E(...) etc. we get the value and a conservative error estimate.

function	defining formulae	command
interval $J = (s_1, s_2)$		J = [s1,s2]
interval $J = (s, \infty)$		J = [s,inf]
interval $J = (-\infty, s)$		J = [-inf,s]
$E_2^{(n)}(k; J)$	(2.11)	E(2,k,J,n)
$E_2^{(n)}((k,0); J_1, J_2)$	(8.15)	E(2,[k,0],{J1,J2},n)
$E_2^{(\mathrm{bulk})}(k; J)$	(2.14)	E(2,k,J,'bulk')
$E_2^{(\mathrm{bulk})}((k,0); J_1, J_2)$	(8.15)	E(2,[k,0],{J1,J2},'bulk')
$E_2^{(\mathrm{soft})}(k; J)$	(2.15)	E(2,k,J,'soft')
$E_2^{(\mathrm{soft})}((k,0); J_1, J_2)$	(8.15)	E(2,[k,0],{J1,J2},'soft')
$F(x, y)$	(8.22)	F2Joint(x,y)
$E_4^{(\mathrm{soft})}(k; J)$	(2.16)	E(4,k,J,'soft','MatrixKernel')
$E_{\mathrm{LUE}}^{(n)}(k; J, \alpha)$	(2.36)	E('LUE',k,J,n,alpha)
$E_{\mathrm{LUE}}^{(n)}((k,0); J_1, J_2, \alpha)$	(8.15)	E('LUE',[k,0],{J1,J2},n,alpha)
$E_2^{(\mathrm{hard})}(k; J, \alpha)$	(2.39)	E(2,k,J,'hard',alpha)
$E_2^{(\mathrm{hard})}((k,0); J_1, J_2, \alpha)$	(8.15)	E(2,[k,0],{J1,J2},'hard',alpha)
$E_+(k; s)$	(5.6)	E('+',k,s)
$E_-(k; s)$	(5.6)	E('-',k,s)
$E_\beta(k; s)$	(2.5), (5.7), (5.8), (5.9)	E(beta,k,s)
$\tilde{E}_+(k; s)$	(6.6)	E('+',k,s,'soft')
$\tilde{E}_-(k; s)$	(6.6)	E('-',k,s,'soft')
$\tilde{E}_\beta(k; s)$	(6.2), (6.7), (6.9), (6.17)	E(beta,k,s,'soft')
$F_\beta(k; s)$	(2.9), (6.1)	F(beta,k,s)
$F_\beta(s)$	(2.10)	F(beta,s)
$E_{+,\alpha}(k; s)$	(7.6)	E('+',k,s,'hard',alpha)
$E_{-,\alpha}(k; s)$	(7.6)	E('-',k,s,'hard',alpha)
$E_{\beta,\alpha}(k; s)$	(7.2), (7.7), (7.9), (7.15)	E(beta,k,s,'hard',alpha)
$F_{\beta,\alpha}(k; s)$	(7.1)	F(beta,k,s,alpha)

```
>> pref('printmode','round');
>> s = 2.13; beta = 1;
>> mass = 0; errmass = 0; mean = 0; errmean = 0;
>> M = 10; for k=0:M
>>    [val,err] = E(beta,k,s);
>>    mass = mass+val; errmass = errmass+err;
>>    mean = mean+k*val; errmean = errmean+k*err;
>> end
>> PrintCorrectDigits(mass,errmass);

   1.0000000000000_

>> PrintCorrectDigits(mean,errmean);

   2.130000000000__
```

The results of (2.8) are perfectly matched. The reader is invited to repeat this experiment with a larger truncation index for the series.

9.3.3. *Example: more general constraints.* The preceding example can be extended to more general probabilities $E(k; J)$ that are given by a determinantal expression of the form (8.14), that is,

$$E(k; J) = \frac{(-1)^k}{k!} \frac{d^k}{dz^k} \det \left(I - zK \restriction_{L^2(J)} \right) \Bigg|_{z=1}, \tag{9.1}$$

for some trace class operator $K \restriction_{L^2(J)}$. Expanding the entire function

$$d(z) = \det \left(I - zK \restriction_{L^2(J)} \right) \tag{9.2}$$

into a power series at $z = 1$ yields

$$\sum_{k=0}^{\infty} E(k; J) = \sum_{k=0}^{\infty} \frac{(-1)^k}{k!} d^{(k)}(1) = d(0) = 1, \tag{9.3a}$$

$$\sum_{k=0}^{\infty} k \, E(k; J) = -\sum_{k=0}^{\infty} \frac{(-1)^k}{k!} d^{(k+1)}(1) = -d'(0) = \text{tr} \left(K \restriction_{L^2(J)} \right); \tag{9.3b}$$

both of which have a probabilistic interpretation (see Deift 1999b, p. 119). Now, for the Airy kernel we get

$$\text{tr} \left(K_{\text{Ai}} \restriction_{L^2(s,\infty)} \right) = \int_s^{\infty} K_{\text{Ai}}(x, x) \, dx$$

$$= \tfrac{1}{3} (2s^2 \text{Ai}(s)^2 - 2s\text{Ai}'(s)^2 - \text{Ai}(s)\text{Ai}'(s)), \tag{9.4}$$

with the specific value (for $s = 0$)

$$\text{tr} \left(K_{\text{Ai}} \restriction_{L^2(0,\infty)} \right) = \frac{1}{9\Gamma(\frac{1}{3})\Gamma(\frac{2}{3})}. \tag{9.5}$$

Now, let us check the quality of the numerical evaluation of (9.3) (and the automatic error control) using this value.

```
>> pref('printmode','round');
>> s = 0; beta = 2;
>> mass = 0; errmass = 0; mean = 0; errmean = 0;
>> M = 3; for k=0:M
>>     [val,err] = E(beta,k,s,'soft');
>>     mass = mass+val; errmass = errmass+err;
>>     mean = mean+k*val; errmean = errmean+k*err;
>> end
>> PrintCorrectDigits(mass,errmass);

   1.000000000000__

>> PrintCorrectDigits(mean,errmean);

   0.030629383079___

>> 1/9/gamma(1/3)/gamma(2/3)

   0.0306293830789884
```

The results are in perfect match with (9.3): they are correctly *rounded*, indeed. The reader is invited to play with the truncation index of the series.

9.3.4. *Example: calculating quantiles.* Quantiles are easy to compute; here come the 5% and 95% quantiles of the Tracy–Widom distribution for GOE:

```
>> F1inv = vec(@(p) (fzero(@(s) F(1,s)-p,0)));
>> F1inv([0.05 0.95])

   -3.18037997693773        0.979316053469556
```

9.4. **Densities and Moments.** Probability densities and moments are computed by barycentric interpolation in m Chebyshev points as described in Section 4.5. This is most conveniently done by installing the functionality of the chebfun package (Trefethen, Pachón, Platte and Driscoll 2008). Our basic command is then, for a given cumulative distribution function $F(s)$:

```
>> [val,err,supp,PDF,CDF] = moments(@(s) F(s),m);
```

If one skips the argument m, the number of points will be chosen automatically. The results are: val gives the first four moments, that is, mean, variance, skewness, and kurtosis of the distribution; err gives the absolute errors of each of those moments; supp gives the numerical support of the density; PDF gives the interpolant (4.13) of the probability density function $F'(s)$ in form of a chebfun object; CDF gives the same for the function $F(s)$ itself. If one sets

```
>> pref('plot',true);
```

a call of the command moments will plot the PDF and the CDF in passing.

9.4.1. *Example: the first four moments of the Tracy–Widom distributions for GOE, GUE, and GSE.* The following fills in the missing high-precision digits for the GSE in Tracy and Widom (2008, Table 1); Figure 8 is automatically generated in passing:
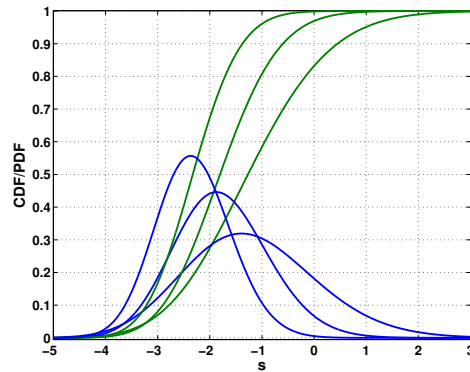
FIGURE 8. Probability density functions $F'_\beta(s)$ (PDF, blue) and cumulative distribution functions $F_\beta(s)$ (CDF, green) of the Tracy–Widom distributions (2.10) for GOE ($\beta = 1$), GUE ($\beta = 2$), and GSE ($\beta = 4$); larger β go to the left. This plot was automatically generated by the commands in Example 9.4.1. Compare with Tracy and Widom (1996, Fig. 1) and Dieng (2005, Fig. 1.1).

```
>> pref('printmode','trunc'); pref('plot',true);
>> for beta = [1 2 4]
>>     [val,err] = moments(@(s) F(beta,s), 128);
>>     PrintCorrectDigits(val,err);
>> end

 -1.2065335745820_   1.607781034581__   0.29346452408____   0.1652429384_____
 -1.771086807411__   0.8131947928329__  0.224084203610___   0.0934480876_____
 -2.306884893241__   0.5177237207726__  0.16550949435____   0.0491951565_____
```

9.4.2. *Example: checking the k-level spacing functions against a constraint.* In the final example of this paper we check our automatic error control in dealing with densities. We take the level spacing densities defined in (2.6) and evaluate the integral constraints (2.7):

```
>> pref('printmode','round'); beta = 1; M = 10; [dom,s] = domain(0,M);
>> E0 = chebfun(vec(@(s) E(beta,0,s)),dom);
>> E1 = chebfun(vec(@(s) E(beta,1,s)),dom);
>> E2 = chebfun(vec(@(s) E(beta,2,s)),dom);
>> p2 = diff(3*E0+2*E1+E2,2);
>> mass = sum(p2); errmass = cheberr(p2);
>> mean = sum(s.*p2); errmean = errmass*sum(s);
>> PrintCorrectDigits(mass,errmass);

   1.0000000000____

>> PrintCorrectDigits(mean,errmean);

   3.000000000_____
```

Once more, the results of (2.7) are perfectly matched. The reader is invited to repeat this experiment with a larger truncation point for the integrals.

A. Appendices

A.1. **Algebraic Kernel Singularities and Gauss–Jacobi Quadrature.** If the kernel is not analytic in a complex neighborhood of the interval defining the integral operator, the straightforward use of the method of Section 4.1, based on Clenshaw–Curtis quadrature, does not generally yield exponential convergence. Since the software limits the number of quadrature points (default is a maximum of 256) this will result in rather inaccurate results (inaccuracies which are detected, however, by the automatic error control). This remark applies in particular to the Laguerre kernel $K_{n,\alpha}(x,y)$ and the Bessel kernel $K_\alpha(x,y)$ which, for non-integer parameter α, exhibit algebraic singularities at $x = 0$ or $y = 0$, namely

$$K_{n,\alpha}(x,y) \propto x^{\alpha/2} \quad (x \to 0), \qquad K_\alpha(x,y) \propto x^{\alpha/2} \quad (x \to 0), \tag{A.1a}$$

$$K_{n,\alpha}(x,y) \propto y^{\alpha/2} \quad (y \to 0), \qquad K_\alpha(x,y) \propto y^{\alpha/2} \quad (y \to 0). \tag{A.1b}$$

A.1.1. *Example: level spacing at the hard edge for non-integer parameter.* Hence, for example, if we want to evaluate the values

$$E_2^{(\text{hard})}\big(1;(0,6),\pm\tfrac{1}{2}\big) = -\frac{d}{dz}\det\left(I - zK_{\pm\frac{1}{2}}\lceil_{L^2(0,6)}\right)\Big|_{z=1},$$

the method of Section 4.1 gives, using Clenshaw–Curtis quadrature, just 1 digit for the stronger singularity $\alpha = -\frac{1}{2}$ and 6 digits for the weaker singularity $\alpha = \frac{1}{2}$:

```
>> pref('quadrature',@ClenshawCurtis); pref('printmode','trunc');
>> s = 6;
>> alpha = -0.5; K.ker = @(x,y) BesselKernel(alpha,x,y); K.mode = 'outer';
>> [val1,err1] = dzdet(op(K,[0,s]),1);
>> alpha =  0.5; K.ker = @(x,y) BesselKernel(alpha,x,y); K.mode = 'outer';
>> [val2,err2] = dzdet(op(K,[0,s]),1);
>> PrintCorrectDigits([val1 val2],[err1 err2]);

   0.8_____    0.524976_____
```

A.1.2. *Gauss–Jacobi quadrature.* This loss of accuracy can be circumvented if we switch from Clenshaw–Curtis quadrature to Gauss–Jacobi quadrature (Szegő 1975, §15.3), which exactly addresses this type of algebraic singularities at the boundary points of the interval. Specifically, this quadrature rule addresses functions f on the interval (a,b) such that, for $\alpha, \beta > -1$, the function $\tilde{f}$ that is obtained from removing the singularities

$$f(x) \propto (x - a)^\alpha \quad (x \to a), \qquad f(x) \propto (b - x)^\beta \quad (x \to b), \tag{A.2}$$

by

$$\tilde{f}(x) = \frac{f(x)}{(x - a)^\alpha (b - x)^\beta} \tag{A.3}$$

is analytic in a complex neighborhood of (a, b). Then, the m-point Gauss–Jacobi quadrature provides nodes $x_j \in (a, b)$ and *positive* weights w_j such that the approximation

$$\sum_{j=1}^{m} w_j f(x_j) \approx \int_a^b f(x) \, dx \tag{A.4}$$

is exponentially convergent: there is a $\rho > 1$ such that the error behaves like $O(\rho^{-m})$ for $m \to \infty$. In our toolbox the Gauss–Jacobi quadrature is called by:

```
>> [w,x] = GaussJacobi(a,b,alpha,beta,m)
```

A.1.3. *Example A.1.1 revisited.* The application of the Gauss–Jacobi quadrature to the Bessel kernel determinant (2.39) requires the determination of the singular exponents that are relevant for the Fredholm determinant. Now, from (A.1) we infer that the eigenfunctions

$$\int_0^s K_\alpha(x, y) u_\lambda(y) \, dy = \lambda u_\lambda(x) \tag{A.5}$$

of the Bessel kernel exhibit the same type of algebraic singularity at $x \to 0$:

$$u_\lambda(x) \propto x^{\alpha/2} \quad (x \to 0). \tag{A.6}$$

It turns out that the singularity of $K_\alpha(x, y) u_\lambda(y)$ at $y \to 0$ governs the behavior of the determinant approximation, that is, we should take the singular exponent of

$$K_\alpha(x, y) u_\lambda(y) \propto y^\alpha \quad (y \to 0). \tag{A.7}$$

Indeed, with this choice of the singular exponent we get 14 digits for both cases:

```
>> alpha = -0.5; pref('quadrature',@(a,b,m) GaussJacobi(a,b,alpha,0,m));
>> K.ker = @(x,y) BesselKernel(alpha,x,y); K.mode = 'outer';
>> [val1,err1] = dzdet(op(K,[0,s]),1);
>> alpha =  0.5; pref('quadrature',@(a,b,m) GaussJacobi(a,b,alpha,0,m));
>> K.ker = @(x,y) BesselKernel(alpha,x,y); K.mode = 'outer';
>> [val2,err2] = dzdet(op(K,[0,s]),1);
>> PrintCorrectDigits([val1 val2],[err1 err2]);

   0.86114217058328_    0.52497677921859_
```

All this is most conveniently hidden from the user who can simply call the high level command that takes care of choosing the appropriate quadrature rule:

```
>> alpha = -0.5; [val1,err1] = E(2,1,[0,s],'hard',alpha);
>> alpha =  0.5; [val2,err2] = E(2,1,[0,s],'hard',alpha);
>> PrintCorrectDigits([val1 val2],[err1 err2]);

   0.86114217058328_    0.52497677921859_
```

Remark. We have studied this particular example because it provides a cross check by the relation

$$E_2^{(\text{hard})}(k; (0, s), \pm\tfrac{1}{2}) = E_\mp(k; 2\sqrt{s}/\pi). \tag{A.8}$$

This relation can be obtained from a simple integral transformation that allows us to rewrite the determinant of the Bessel kernel for $\alpha = \pm\frac{1}{2}$ as that of the odd or even sine kernel. This way (switching back to Clenshaw–Curtis quadrature which

TABLE 7. Statistical properties of $p_1(k;s)$ for various k. Note that because of $p_4(k;s) = 2p_1(2k+1,2s)$ one can read off the values for $p_4(k;s)$ from those for $p_1(2k+1;s)$: Just divide the mean by two and the variance by four, skewness and kurtosis remain unchanged.

PDF	mean	variance	skewness	kurtosis	time
$p_1(0;s)$	1	0.28553 06557	0.68718 99889	0.37123 80638	0.67
$p_1(1;s)$	2	0.41639 36889	0.34939 68438	0.02858 27332	1.22
$p_1(2;s)$	3	0.49745 52604	0.22741 44134	−0.01329 56588	2.59
$p_1(3;s)$	4	0.55564 24180	0.16645 68639	−0.01994 68028	4.24
$p_1(4;s)$	5	0.60091 83521	0.13042 07251	−0.02007 29233	5.81
$p_1(5;s)$	6	0.63794 46245	0.10679 47124	−0.01884 07449	7.43
$p_1(6;s)$	7	0.66925 53948	0.09018 32871	−0.01743 19487	9.46
$p_1(7;s)$	8	0.69637 60657	0.07790 15490	−0.01613 54800	11.04
$p_1(8;s)$	9	0.72029 45046	0.06847 07897	−0.01500 75200	12.80
$p_1(9;s)$	10	0.74168 65573	0.06101 25387	−0.01404 07984	15.26

is appropriate here) we get values that are in perfect agreement with the ones obtained for the Bessel kernel with Gauss–Jacobi quadrature:

```
>> [val1,err1] = E('+',1,2*sqrt(s)/pi);
>> [val2,err2] = E('-',1,2*sqrt(s)/pi);
>> PrintCorrectDigits([val1 val2],[err1 err2])

   0.861142170583288    0.524976779218593
```

A.2. **Tables of Some Statistical Properties.** We provide some tables of statistical properties of the k-level spacing densities $p_\beta(k;s)$, defined in (2.6), and the distributions $F_\beta(k;s)$ of the k-th largest level at the soft edge, defined in (2.9). The tables display correctly *truncated* digits that have passed the automatic error control of the software in Section 9. Computing times are in seconds.

Note that because of the interrelations between GOE and GSE there is no need to separately tabulate the values for $\beta = 4$: first, the interlacing property (6.14) gives $F_4(k;s) = F_1(2k;s)$. Second, we infer from (5.8) and (5.9) that

$$E_4(k;s) = \tfrac{1}{2}E_1(2k-1;2s) + E_1(2k;2s) + \tfrac{1}{2}E_1(2k+1;2s) \tag{A.9}$$

which implies

$$p_4(k;s) = 2p_1(2k+1;2s). \tag{A.10}$$

Acknowledgements

TABLE 8. Statistical properties of p_2 for various k.

PDF	mean	variance	skewness	kurtosis	time
$p_2(0; s)$	1	0.17999 38776	0.49706 36204	0.12669 98480	0.63
$p_2(1; s)$	2	0.24897 77536	0.24167 43158	−0.01494 23984	1.36
$p_2(2; s)$	3	0.29016 98290	0.15542 00591	−0.02317 40428	1.44
$p_2(3; s)$	4	0.31944 35563	0.11334 61773	−0.02150 23114	1.67
$p_2(4; s)$	5	0.34214 08054	0.08871 43069	−0.01914 18388	2.09
$p_2(5; s)$	6	0.36067 45961	0.07263 43907	−0.01714 28515	2.06
$p_2(6; s)$	7	0.37633 63928	0.06135 08835	−0.01555 25979	2.19
$p_2(7; s)$	8	0.38989 74631	0.05301 56552	−0.01428 79010	2.41
$p_2(8; s)$	9	0.40185 51105	0.04661 73337	−0.01326 81121	2.56
$p_2(9; s)$	10	0.41254 86854	0.04155 73856	−0.01243 20513	2.74

TABLE 9. Statistical properties of $F_1(k; s)$ for various k. Note that because of $F_4(k; s) = F_1(2k, s)$ one can directly read off the values for $F_4(k; s)$ from those for $F_1(2k; s)$.

CDF	mean	variance	skewness	kurtosis	time
$F_1(1; s)$	−1.20653 35745	1.60778 10345	0.29346 45240	0.16524 29384	4.59
$F_1(2; s)$	−3.26242 79028	1.03544 74415	0.16550 94943	0.04919 51565	12.45
$F_1(3; s)$	−4.82163 02757	0.82239 01151	0.11762 14761	0.01977 46604	30.04
$F_1(4; s)$	−6.16203 99636	0.70315 81054	0.09232 83954	0.00816 06305	51.24
$F_1(5; s)$	−7.37011 47042	0.62425 23679	0.07653 98210	0.00245 40580	77.49
$F_1(6; s)$	−8.48621 83723	0.56700 71487	0.06567 07705	−0.00073 42515	112.00

TABLE 10. Statistical properties of $F_2(k; s)$ for various k.

CDF	mean	variance	skewness	kurtosis	time
$F_2(1; s)$	−1.77108 68074	0.81319 47928	0.22408 42036	0.09344 80876	1.84
$F_2(2; s)$	−3.67543 72971	0.54054 50473	0.12502 70941	0.02173 96385	5.44
$F_2(3; s)$	−5.17132 31745	0.43348 13326	0.08880 80227	0.00509 66000	10.41
$F_2(4; s)$	−6.47453 77733	0.37213 08147	0.06970 92726	−0.00114 15160	17.89
$F_2(5; s)$	−7.65724 22912	0.33101 06544	0.05777 55438	−0.00405 83706	25.56
$F_2(6; s)$	−8.75452 24419	0.30094 94654	0.04955 14791	−0.00559 98554	34.72

REFERENCES

Adler, M. and van Moerbeke, P.: 2005, PDEs for the joint distributions of the Dyson, Airy and sine processes, *Ann. Probab.* **33**, 1326–1361.

Basor, E. L., Tracy, C. A. and Widom, H.: 1992, Asymptotics of level-spacing distributions for random matrices, *Phys. Rev. Lett.* **69**, 5–8.

Battles, Z. and Trefethen, L. N.: 2004, An extension of MATLAB to continuous functions and operators, *SIAM J. Sci. Comput.* **25**, 1743–1770.

Berrut, J.-P. and Trefethen, L. N.: 2004, Barycentric Lagrange interpolation, *SIAM Rev.* **46**, 501–517.

Bornemann, F.: 2009, Accuracy and stability of computing high-order derivatives of analytic functions by Cauchy integrals, *Found. Comput. Math.* (to appear). e-print: `arXiv:0910.1841v4`.

Bornemann, F.: 2010a, On the numerical evaluation of Fredholm determinants, *Math. Comp.* **79**, 871–915.

Bornemann, F.: 2010b, Asymptotic independence of the extreme eigenvalues of GUE, *J. Math. Phys.* **51**, 023514, 8pp.

Bornemann, F., Ferrari, P. L. and Prähofer, M.: 2008, The $Airy_1$ process is not the limit of the largest eigenvalue in GOE matrix diffusion, *J. Stat. Phys.* **133**, 405–415.

Borodin, A. and Forrester, P. J.: 2003, Increasing subsequences and the hard-to-soft edge transition in matrix ensembles, *J. Phys. A* **36**, 2963–2981.

Borwein, J. and Bailey, D.: 2004, *Mathematics by experiment: Plausible reasoning in the 21st century*, A K Peters, Natick.

Brézin, É. and Kazakov, V. A.: 1990, Exactly solvable field theories of closed strings, *Phys. Lett. B* **236**.

Bronk, B. V.: 1964, Accuracy of the semicircle approximation for the density of eigenvalues of random matrices, *J. Math. Phys.* **5**, 215–220.

Clarkson, P. A.: 2006, Painlevé equations—nonlinear special functions, *Orthogonal polynomials and special functions*, Vol. 1883 of *Lecture Notes in Math.*, Springer, Berlin, pp. 331–411.

Davis, P. J. and Rabinowitz, P.: 1984, *Methods of numerical integration*, 2nd edn, Academic Press, Orlando.

Deift, P.: 1999a, Integrable operators, *Differential operators and spectral theory*, Vol. 189 of *Amer. Math. Soc. Transl. Ser. 2*, Amer. Math. Soc., Providence, pp. 69–84.

Deift, P.: 1999b, *Orthogonal polynomials and random matrices: a Riemann-Hilbert approach*, American Mathematical Society, Providence.

Deift, P.: 2007, Universality for mathematical and physical systems, *International Congress of Mathematicians. Vol. I*, Eur. Math. Soc., Zürich, pp. 125–152.

Desrosiers, P. and Forrester, P. J.: 2006, Relationships between τ-functions and Fredholm determinant expressions for gap probabilities in random matrix theory, *Nonlinearity* **19**, 1643–1656.

Deuflhard, P. and Bornemann, F.: 2002, *Scientific computing with ordinary differential equations*, Springer-Verlag, New York.

Dieng, M.: 2005, *Distribution Functions for Edge Eigenvalues in Orthogonal and Symplectic Ensembles: Painlevé Representations*, PhD thesis, University of Davis. e-print: `arXiv:math/0506586v2`.

Driscoll, T. A., Bornemann, F. and Trefethen, L. N.: 2008, The chebop system for automatic solution of differential equations, *BIT* **48**, 701–723.

Dyson, F. J.: 1962, Statistical theory of the energy levels of complex systems. III, *J. Mathematical Phys.* **3**, 166–175.

Edelman, A. and Persson, P.-O.: 2005, Numerical methods for eigenvalue distributions of random matrices. e-print: `arXiv:math-ph/0501068v1`.

Edelman, A. and Rao, N. R.: 2005, Random matrix theory, *Acta Numer.* **14**, 233–297.

Ferrari, P. L. and Spohn, H.: 2005, A determinantal formula for the GOE Tracy-Widom distribution, *J. Phys. A* **38**, L557–L561.

Fokas, A. S., Its, A. R., Kapaev, A. A. and Novokshenov, V. Y.: 2006, *Painlevé transcendents: The Riemann-Hilbert approach*, American Mathematical Society, Providence.

Forrester, P. J.: 1993, The spectrum edge of random matrix ensembles, *Nuclear Phys. B* **402**, 709–728.

Forrester, P. J.: 2006, Hard and soft edge spacing distributions for random matrix ensembles with orthogonal and symplectic symmetry, *Nonlinearity* **19**, 2989–3002.

Forrester, P. J. and Rains, E. M.: 2001, Interrelationships between orthogonal, unitary and symplectic matrix ensembles, *Random matrix models and their applications*, Vol. 40 of *Math. Sci. Res. Inst. Publ.*, Cambridge Univ. Press, Cambridge, pp. 171–207.

Forrester, P. J. and Witte, N. S.: 2002, Application of the τ-function theory of Painlevé equations to random matrices: P_V, P_{III}, the LUE, JUE, and CUE, *Comm. Pure Appl. Math.* **55**, 679–727.

Gaudin, M.: 1961, Sur la loi limite de l'espacement des valeurs propres d'une matrice aléatoire, *Nucl. Phys.* **25**, 447–458.

Gohberg, I., Goldberg, S. and Krupnik, N.: 2000, *Traces and determinants of linear operators*, Birkhäuser Verlag, Basel.

Hägg, J.: 2008, Local Gaussian fluctuations in the Airy and discrete PNG processes, *Ann. Probab.* **36**, 1059–1092.

Hastings, S. P. and McLeod, J. B.: 1980, A boundary value problem associated with the second Painlevé transcendent and the Korteweg-de Vries equation, *Arch. Rational Mech. Anal.* **73**, 31–51.

Higham, N. J.: 2004, The numerical stability of barycentric Lagrange interpolation, *IMA J. Numer. Anal.* **24**, 547–556.

Jimbo, M., Miwa, T., Môri, Y. and Sato, M.: 1980, Density matrix of an impenetrable Bose gas and the fifth Painlevé transcendent, *Phys. D* **1**, 80–158.

Kahn, P. B.: 1963, Energy level spacing distributions, *Nucl. Phys.* **41**, 151–166.

Mehta, M. L.: 2004, *Random matrices*, 3rd edn, Elsevier/Academic Press, Amsterdam.

Mehta, M. L. and des Cloizeaux, J.: 1972, The probabilities for several consecutive eigenvalues of a random matrix, *Indian J. Pure Appl. Math.* **3**, 329–351.

Moore, G.: 1990, Matrix models of 2D gravity and isomonodromic deformation, *Progr. Theoret. Phys. Suppl.* (102), 255–285.

Odlyzko, A. M.: 1987, On the distribution of spacings between zeros of the zeta function, *Math. Comp.* **48**, 273–308.

Olver, F. W. J.: 1974, *Asymptotics and special functions*, Academic Press, New York, London.

Prähofer, M.: 2003, Tables to: Exact scaling functions for one-dimensional stationary KPZ growth. `http://www-m5.ma.tum.de/KPZ/`.

Prähofer, M. and Spohn, H.: 2002, Scale invariance of the PNG droplet and the Airy process, *J. Statist. Phys.* **108**, 1071–1106.

Prähofer, M. and Spohn, H.: 2004, Exact scaling functions for one-dimensional stationary KPZ growth, *J. Statist. Phys.* **115**, 255–279.

Salzer, H. E.: 1972, Lagrangian interpolation at the Chebyshev points $X_{n,\nu} \equiv \cos(\nu\pi/n)$, $\nu = 0(1)n$; some unnoted advantages, *Comput. J.* **15**, 156–159.

Simon, B.: 2005, *Trace ideals and their applications*, 2nd edn, American Mathematical Society, Providence.

Stewart, G. W.: 1998, *Matrix algorithms. Vol. I: Basic decompositions*, Society for Industrial and Applied Mathematics, Philadelphia.

Stratton, J. A., Morse, P. M., Chu, L. J., Little, J. D. C. and Corbató, F. J.: 1956, *Spheroidal wave functions, including tables of separation constants and coefficients*, John Wiley & Sons, New York.

Szegő, G.: 1975, *Orthogonal polynomials*, 4th edn, American Mathematical Society, Providence.

Tracy, C. A. and Widom, H.: 1993a, Introduction to random matrices, *Geometric and quantum aspects of integrable systems*, Vol. 424 of *Lecture Notes in Phys.*, Springer, Berlin, pp. 103–130.

Tracy, C. A. and Widom, H.: 1993b, Level-spacing distributions and the Airy kernel, *Phys. Lett. B* **305**, 115–118.

Tracy, C. A. and Widom, H.: 1994a, Level-spacing distributions and the Airy kernel, *Comm. Math. Phys.* **159**, 151–174.

Tracy, C. A. and Widom, H.: 1994b, Level spacing distributions and the Bessel kernel, *Comm. Math. Phys.* **161**, 289–309.

Tracy, C. A. and Widom, H.: 1994c, Fredholm determinants, differential equations and matrix models, *Comm. Math. Phys.* **163**, 33–72.

Tracy, C. A. and Widom, H.: 1996, On orthogonal and symplectic matrix ensembles, *Comm. Math. Phys.* **177**, 727–754.

Tracy, C. A. and Widom, H.: 1998, Correlation functions, cluster functions, and spacing distributions for random matrices, *J. Statist. Phys.* **92**, 809–835.

Tracy, C. A. and Widom, H.: 2000, Universality of the distribution functions of random matrix theory, *Integrable systems: from classical to quantum (Montréal, QC, 1999)*, Vol. 26 of *CRM Proc. Lecture Notes*, Amer. Math. Soc., Providence, pp. 251–264.

Tracy, C. A. and Widom, H.: 2005, Matrix kernels for the Gaussian orthogonal and symplectic ensembles, *Ann. Inst. Fourier (Grenoble)* **55**, 2197–2207.

Tracy, C. A. and Widom, H.: 2008, The distributions of random matrix theory and their applications. `http://www.math.ucdavis.edu/~tracy/talks/SITE7.pdf`.

Trefethen, L. N., Pachón, R., Platte, R. B. and Driscoll, T. A.: 2008, The chebfun project: computing with functions instead of numbers. Version 3. Oxford University Mathematical Institute. `http://www2.maths.ox.ac.uk/chebfun/`.

Widom, H.: 2004, On asymptotics for the Airy process, *J. Statist. Phys.* **115**, 1129–1134.

Wu, T. T., McCoy, B. M., Tracy, C. A. and Barouch, E.: 1976, Spin-spin correlation functions for the two-dimensional Ising model: Exact theory in the scaling region, *Phys. Rev. B* **13**, 316–374.

Zentrum Mathematik – M3, Technische Universität München, 80290 München, Germany
E-mail address: bornemann@ma.tum.de